The Ensemble Kalman Filter for Combined State and Parameter Estimation

MONTE CARLO TECHNIQUES FOR DATA ASSIMILATION IN LARGE SYSTEMS

GEIR EVENSEN

The ensemble Kalman filter (EnKF) [1] is a sequential Monte Carlo method that provides an alternative to the traditional Kalman filter (KF) [2], [3] and adjoint or four-dimensional variational (4DVAR) methods [4]–[6] to better handle large state spaces and nonlinear error evolution. EnKF provides a simple conceptual formulation and ease of implementation, since

Frontiers of Data Assimilation

PHOTO COMPOSITE COURTESY OF DAVID STENSRUD

there is no need to derive a tangent linear operator or adjoint equations, and there are no integrations backward in time. EnKF is used extensively in a large community, including ocean and atmospheric sciences, oil reservoir simulations, and hydrological modeling.

To a large extent EnKF overcomes two problems associated with the traditional KF. First, in KF an error covariance matrix for the model state needs to be stored and propagated in time, making the method computationally infeasible for models with high-dimensional state vectors. Second, when the model dynamics are nonlinear, the extended KF (EKF) uses a linearized equation for the error covariance evolution, and this linearization can result in unbounded linear instabilities for the error evolution [7].

In contrast with EKF, EnKF represents the error covariance matrix by a large stochastic ensemble of model realizations. For large systems, the dimensionality problem is managed by using a low-rank approximation of the error covariance matrix, where the number of independent model realizations is less than the number of unknowns in the model. Thus, the uncertainty is represented by a set of model realizations rather than an explicit expression for the error covariance matrix. The ensemble of model states is integrated forward in time to predict error statistics. For linear models the ensemble integration is consistent with the exact integration of an error covariance equation in the limit of an infinite ensemble size. Furthermore, for nonlinear dynamical models, the use of an ensemble integration leads to full nonlinear evolution of the error statistics, which in EnKF can be computed with a much lower computational cost than in EKF [8].

Whenever measurements are available, each individual realization is updated to incorporate the new information provided by the measurements. Implementations of the update schemes can be formulated as either a stochastic [9] or a deterministic scheme [8], [10]–[13]. Both kinds of schemes solve for a variance-minimizing solution and implicitly assume that the forecast error statistics are Gaussian by using only the ensemble covariance in the update equation.

The assumption of Gaussian distributions in EnKF allows for a linear and efficient update equation to be used. A more sophisticated update scheme needs to be derived to take into account higher order statistics, which leads to particle filtering theory [14], where the Bayes formula is solved at each update step, although normally at a huge computational cost. While the particle filter accounts for non-Gaussian distributions by representing the full pdf in the parameter space, its applicability is normally limited to estimation of a few unknowns at the cost of integrating a very large ensemble consisting of typically more than $\mathcal{O}(10^4)$ realizations.

In [8], EnKF is rederived as a sequential Monte Carlo method starting from a Bayesian formulation. The EnKF can then be characterized as a special case of the particle filter, where the Bayesian update step in the particle filter is approximated with a linear update step in the EnKF using only the two first moments of the predicted probability density function (pdf). With linear dynamics, EnKF is equivalent to a particle filter, since this case is fully described by Gaussian pdfs. However, with nonlinear dynamics, non-Gaussian contributions may develop, and the EnKF only approximates the particle filter. Unlike the particle filters [14], EnKF does not need to re-sample the ensemble from the posterior pdf during the analysis step, since each prior model realization is individually updated to create the correct posterior ensemble.

In EnKF, the solution is solved for in the affine space spanned by the ensemble of realizations. The ensemble, which evolves in time according to the nonlinear dynamical model, provides a representation of the subspace where the update is computed at each analysis time. It is possible to formulate analysis schemes in terms of the ensemble, leading to efficient algorithms where the state error covariance matrix is not computed and is only implicitly used.

A major approximation introduced in EnKF is related to the use of a limited number of ensemble realizations. The ensemble size limits the space where the solution is searched for and in addition introduces spurious correlations that lead to excessive decrease of the ensemble variance and possibly filter divergence. The spurious correlations can be handled by localization methods that attempt to reduce the impact of measurements that are located far from the gridpoint to be updated. Localization methods either filter away distant measurements or attempt to reduce the amplitude of the long-range spurious correlations. The use of a local analysis scheme effectively increases the ensemble solution space while reducing the impact of spurious correlations. The use of a local analysis scheme allows for a relatively small ensemble size to be used with a high-dimensional dynamical model.

A chronological list of applications of EnKF is given in [8]. This list includes both low-dimensional systems of highly nonlinear dynamical models as well as high-dimensional ocean and atmospheric circulation models with $\mathcal{O}(10^6)$ or more unknowns. Applications include state estimation in operational circulation models for the ocean and atmosphere as well as parameter estimation or history matching in reservoir simulation models. For example, [15]–[17] present an implementation of an EnKF with an isopycnal ocean general circulation model, while [18] examines an implementation of a local EnKF with a state-of-the-art operational numerical weather prediction model using simulated measurements. It is shown that a modest-sized ensemble of 40 members can track the evolution of the atmospheric state with high accuracy.

An implementation of the EnKF at the Canadian Meteorological Centre in [19] demonstrates EnKF for operational atmospheric data assimilation and reviews EnKF with focus on localization and sampling errors. A review in [20] of a variant of EnKF called the local ensemble transform Kalman filter includes a derivation of the analysis equations and the numerical implementation, which differ somewhat from what is normally used in the Kalman filtering literature. An implementation of the local ensemble transform Kalman filter with the National Centers for Environmental Prediction (NCEP) global model, given in [21], concludes that the accuracy of the method is competitive with operational algorithms and that this technique can efficiently handle large number of measurements.

An implementation of EnKF with the NCEP model in [22] is compared with the operational NCEP global data assimilation system. The ensemble data assimilation system outperforms a reduced-resolution version of the operational three-dimensional variational (3DVAR) data assimilation

system and shows improvement in data sparse regions. An observation-thinning algorithm is presented in [22], where observations with little information content leading to low variance reduction are filtered out. The thinning algorithm improves the analysis when unmodeled error correlations are present between nearby observations. The need for the thinning is eliminated if the error correlations are properly specified in the measurement error covariance matrix.

EnKF is currently used in several research fields in addition to the ocean and atmosphere applications cited throughout this article. In [23], the EnKF is used to update a model of tropospheric ozone concentrations and to compute short-term air quality forecasts. It is found that the EnKF updated estimates provide improved initial conditions and lead to better forecasts of the next day's ozone concentration maxima. In [24], EnKF is applied to a magnetohydrodynamic model for space weather prediction. The performance of EnKF in a land surface data assimilation experiment is examined in [25]. These results are compared with a sequential importance re-sampling (SIR) filter, and it is found that EnKF performs almost as well as the SIR filter. Furthermore, it is emphasized that EnKF leads to skewed and even multimodal distributions despite the normality assumption imposed when computing the analysis updates.

In this article, we outline the theory behind the EnKF and demonstrate its use in various high-dimensional and nonlinear applications in mathematical physics while also considering the combined parameter and state estimation problem in some detail. The goal of this article is to serve as an introduction and tutorial for new users of EnKF. We thus present examples that illustrate particular properties of the EnKF, such as its capability to handle high-dimensional state spaces as well as highly nonlinear dynamics.

DATA ASSIMILATION AND PARAMETER ESTIMATION

Given a dynamical model with initial and boundary conditions and a set of measurements that can be related to the model state, the state estimation problem is defined as finding the estimate of the model state that in some weighted measure best fits the model equations, the initial and boundary conditions, and the observed data. Unless we relax the equations and allow some or all of the dynamical model, the conditions, and the measurements to contain errors, the problem may become overdetermined and no general solution exists.

We often use a prior assumption of Gaussian distributions for the error terms. It is also common to assume that errors in the measurements are uncorrelated with errors in the dynamical model. The problem can then be formulated by using a quadratic cost function whose minimum defines the best estimate of the state.

The parameter estimation problem is different from the state estimation problem. Traditionally, in parameter estimation we want to improve estimates of a set of poorly known model parameters leading to an exact model solution that is close to the measurements. Thus, in this case we assume that all errors in the model equations are associated with uncertainties in the selected model parameters. The model initial conditions, boundary conditions, and the model structure are all exactly known. Thus, for any set of model parameters the corresponding solution is found from a single forward integration of the model. The way forward is then to define a cost function that measures the distance between the model prediction and the observations plus a term measuring the deviation of the parameter values from a prior estimate of the parameter values. The relative weight between these two terms is determined by the prior error statistics for the measurements and the prior parameter estimate. Unfortunately, these problems are often hard to solve [8] since the inverse problem is highly nonlinear, and multiple local minima may be present in the cost function.

In [8] the combined parameter and state estimation problem is considered. An improved state estimate and a set of improved model parameters are then searched for simultaneously. In [26] and [27] this problem is formulated using a variational cost function that is minimized using the representer method [28], [29]. Both [26] and [27] report convergence problems due to the nonlinearity of the problem and the possible presence of multiple local minima in the cost function. In [8] it is shown that the combined parameter and state estimation problem can be formulated, and in many cases solved efficiently, using ensemble methods. An illustrative application of the EnKF for combined state and parameter estimation includes estimation of the permeability fields together with dynamic state variables in reservoir simulation models [30]. These problems have huge parameter and state spaces with $\mathcal{O}(10^6)$ unknowns. The formulation and solution of the combined parameter and state estimation problem using ensemble methods are further discussed below.

REVIEW OF THE KALMAN FILTER

Variance Minimizing Analysis Scheme

The KF is a variance-minimizing algorithm that updates the state estimate whenever measurements are available. The update equations in the KF are normally derived by minimizing the trace of the posterior error covariance matrix. The algorithm refers only to first- and second-order statistical moments. With the assumption of Gaussian priors for the model prediction and the data, the update equation can also be derived as the minimizing solution of a quadratic cost function. We start with a vector of variables stored in $\psi(x, t)$, which is defined on some spatial domain $\partial \mathcal{D}$ with spatial coordinate x. When $\psi(x, t)$ is discretized on a numerical grid representing the spatial

model domain, it can be represented by the state vector ψ_k at each time instant t_k. The cost function can then be written as

$$\mathcal{J}[\psi_k^a] = (\psi_k^f - \psi_k^a)^\mathrm{T} (C_{\psi\psi}^f)_k^{-1} (\psi_k^f - \psi_k^a)$$
$$+ (d_k - M_k\psi_k^a)^\mathrm{T} (C_{\epsilon\epsilon})_k^{-1} (d_k - M_k\psi_k^a), \quad (1)$$

where ψ_k^a and ψ_k^f are the analyzed and forecast estimates respectively, d_k is the vector of measurements, M_k is the measurement operator that maps the model state ψ_k to the measurements d_k, $(C_{\psi\psi}^f)_k$ is the error covariance of the predicted model state, and $(C_{\epsilon\epsilon})_k$ is the measurement error covariance matrix. Minimizing with respect to ψ_k^a yields the classical KF update equations

$$\psi_k^a = \psi_k^f + K_k(d_k - M_k\psi_k^f), \quad (2)$$
$$(C_{\psi\psi})_k^a = (I - K_k M_k)(C_{\psi\psi})_k^f, \quad (3)$$
$$K_k = (C_{\psi\psi})_k^f M_k^\mathrm{T} (M_k(C_{\psi\psi})_k^f M_k^\mathrm{T} + (C_{\epsilon\epsilon})_k)^{-1}, \quad (4)$$

where the matrix K_k is the Kalman gain. Thus, both the model state and its error covariance are updated.

Kalman Filter

It is assumed that the true state ψ^t evolves in time according to the dynamical model

$$\psi_k^t = F\psi_{k-1}^t + q_{k-1}, \quad (5)$$

where F is a linear model operator and q_{k-1} is the unknown model error over one time step from $k-1$ to k. In this case a numerical model evolves according to

$$\psi_k^f = F\psi_{k-1}^a, \quad (6)$$

where the superscripts a and f denote analysis and forecast. That is, given the best possible estimate (traditionally named analysis) for ψ at time t_{k-1}, a forecast is calculated at time t_k, using the approximate equation (6).

The error covariance equation is derived by subtracting (6) from (5), squaring the result, and taking the expectation, which yields

$$C_{\psi\psi}^f(t_k) = F C_{\psi\psi}^a(t_{k-1}) F^\mathrm{T} + C_{qq}(t_{k-1}), \quad (7)$$

where we define the error covariance matrices for the predicted and analyzed estimates as

$$C_{\psi\psi}^f = \overline{(\psi^f - \psi^t)(\psi^f - \psi^t)^\mathrm{T}}, \quad (8)$$
$$C_{\psi\psi}^a = \overline{(\psi^a - \psi^t)(\psi^a - \psi^t)^\mathrm{T}}. \quad (9)$$

The overline denotes an expectation operator, which is equivalent to averaging over an ensemble of infinite size.

Extended Kalman Filter

We now assume a nonlinear model, where the true state vector ψ_k^t at time t_k is calculated from

$$\psi_k^t = G(\psi_{k-1}^t) + q_{k-1}, \quad (10)$$

and a forecast is calculated from the approximate equation

$$\psi_k^f = G(\psi_{k-1}^a). \quad (11)$$

The error statistics then evolve according to the equation

$$C_{\psi\psi}^f(t_k) = G_{k-1}' C_{\psi\psi}^a(t_{k-1}) G_{k-1}'^\mathrm{T} + C_{qq}(t_{k-1}) + \cdots, \quad (12)$$

where $C_{qq}(t_{k-1})$ is the model error covariance matrix and G_{k-1}' is the Jacobian or tangent linear operator given by

$$G_{k-1}' = \left. \frac{\partial G(\psi)}{\partial \psi} \right|_{\psi_{k-1}}. \quad (13)$$

Note that in (12) we neglect an infinite number of terms containing higher order statistical moments and higher order derivatives of the model operator. EKF is based on the assumption that the contributions from all of the higher order terms are negligible. By discarding these terms we are left with the approximate error covariance expression

$$C_{\psi\psi}^f(t_k) \simeq G_{k-1}' C_{\psi\psi}^a(t_{k-1}) G_{k-1}'^\mathrm{T} + C_{qq}(t_{k-1}). \quad (14)$$

Higher order approximations for the error covariance evolution are discussed in [31].

EKF with a Nonlinear Ocean Circulation Model

As an application of EKF we consider a nonlinear ocean circulation model [7]. The model in Figure 1 is a multilayer quasi-geostrophic model of the mesoscale ocean currents. The quasi-geostrophic model solves simplified fluid equations for the slow motions in the ocean and are formulated in terms of potential vorticity advection in a background velocity field represented by a stream function. Given a change in the vorticity field, at each time step we can solve for the corresponding stream function.

It is found that the linear evolution equation for the error covariance matrix leads to a linear instability. This instability is demonstrated in an experiment using a steady background flow defined by an eddy standing on a flat bathymetry [see Figure 1(a)]. This particular stream function results in a velocity shear and thus supports a sheared flow instability. Thus, if we add a perturbation and advect it using the linearized equations, then the perturbation grows exponentially. This growth is exactly what is observed in Figure 1(b) and (c). By choosing an initial variance equal to one throughout the model domain, we observe strong

error-variance growth at locations of large velocity and velocity shear in the eddy. The estimated mean square errors, which equal the trace of $C_{\psi\psi}$ divided by the number of gridpoints, indicate exponential error-variance growth.

This linear instability is not realistic. In the real world we expect the instability to saturate at a certain climatological amplitude. As an example, in the atmosphere it is always possible to define a maximum and minimum pressure, which is never exceeded, and the same applies for the eddy field in the ocean. An unstable variance growth cannot be accepted but is in fact what the EKF provides in some cases.

Thus, an apparent closure problem is present in the error-covariance evolution equation, caused by discarding third- and higher order moments in the error covariance equation, leading to a linear instability. If a correct equation could be used to predict the time evolution of the errors, then linear instabilities would saturate due to nonlinear effects. This saturation is missing in EKF, as confirmed by [32]–[34].
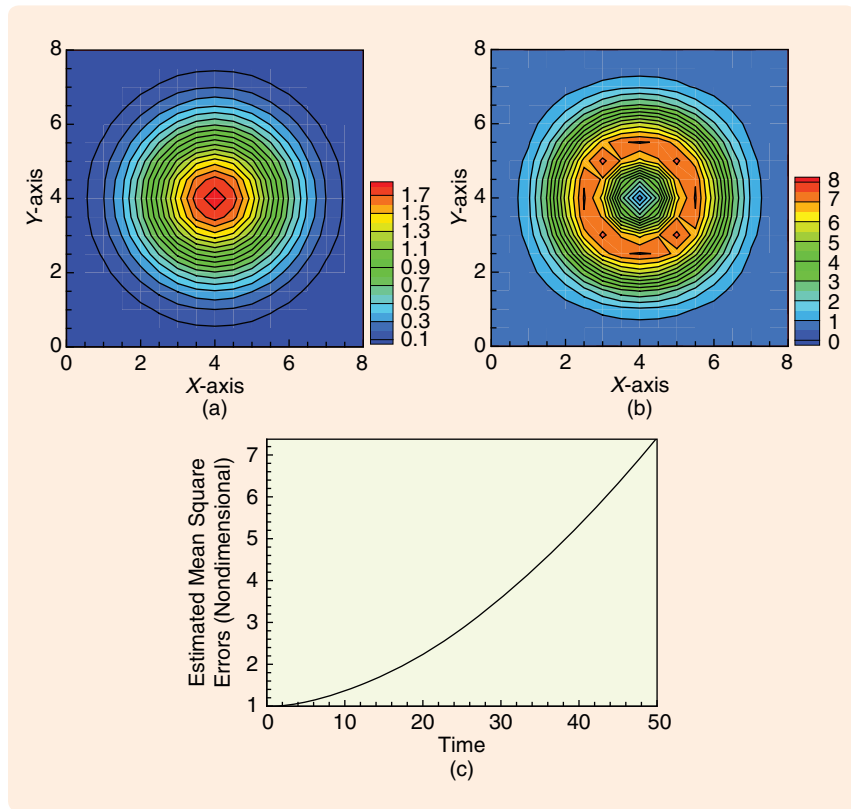

FIGURE 1 Example of an extended Kalman filter experiment from [7]. (a) shows the stream function defining the velocity field of a stationary eddy, while (b) shows the resulting error variance in the model domain after integration from $t = 0$ to $t = 25$. Note the large errors at locations where velocities are high. (c) shows the exponential time evolution of the estimated variance averaged over the model domain.

Extended Kalman Filter for the Mean

Equations (11), (13), and (14) are the most commonly used for EKF. A weakness of the formulation is that the central forecast is used as the estimate. The central forecast is the single model realization initialized with the expected value of the initial state and then integrated by the dynamical model and updated at the measurement steps. For nonlinear dynamics the central forecast may not be equal to the expected value, and thus it is just one realization from an infinite ensemble of possible realizations.

An alternative approach is to derive a model for the evolution of the first moment or mean. First $G(\psi)$ is expanded around $\overline{\psi}$ to obtain

$$G(\psi) = G(\overline{\psi}) + G'(\overline{\psi})(\psi - \overline{\psi}) + \frac{1}{2}G''(\overline{\psi})(\psi - \overline{\psi})^2 + \cdots. \tag{15}$$

Inserting (15) in (11) and taking the expectation or ensemble average yields

$$\overline{\psi_k} = G(\overline{\psi_{k-1}}) + \frac{1}{2}G''_{k-1}C_{\psi\psi}(t_{k-1}) + \cdots. \tag{16}$$

It can be argued that for a statistical estimator it makes more sense to work with the mean than a central forecast. After all, the central forecast does not have any statistical interpretation as illustrated by running an atmospheric model without assimilation updates. The central forecast then becomes just one realization out of infinitely many possible realizations, and it is not clear how we can relate the central forecast to the climatological error covariance estimate. On the other hand the equation for the mean provides an estimate that converges to the climatological mean, and the covariance estimate thus describes the error variance of the climatological mean. All applications of the EKF for data assimilation in ocean and atmospheric models use an equation for the central forecast. However, the interpretation using the equation for the mean supports the formulation used in EnKF.

ENSEMBLE KALMAN FILTER

We begin by representing the error statistics using an ensemble of model states. Next, we present an alternative to the traditional error covariance equation for predicting error statistics. Finally, we derive the traditional EnKF analysis scheme.

Representation of Error Statistics

The error covariance matrices $C_{\psi\psi}^f$ and $C_{\psi\psi}^a$ for the predicted and analyzed estimate in the Kalman filter are defined in terms of the true state in (8) and (9). However, since the true state is not known, we define the ensemble covariance matrices around the ensemble mean $\overline{\psi}$ according to

$$(C_{\psi\psi}^e)^f = \overline{(\psi^f - \overline{\psi^f})(\psi^f - \overline{\psi^f})^T}, \qquad (17)$$

$$(C_{\psi\psi}^e)^a = \overline{(\psi^a - \overline{\psi^a})(\psi^a - \overline{\psi^a})^T}, \qquad (18)$$

where now the overline denotes an average over the ensemble. Thus, we can use an interpretation where the ensemble mean is the best estimate and the spreading of the ensemble around the mean is a natural definition of the error in the ensemble mean.

Thus, instead of storing a full covariance matrix, we can represent the same error statistics using an appropriate ensemble of model states. Given an error covariance matrix, an ensemble of finite size provides an approximation to the error covariance matrix, and, as the size N of the ensemble increases, the errors in the Monte Carlo sampling decrease proportionally to $1/\sqrt{N}$.

Suppose now that we have N model states or realizations in the ensemble, each of dimension n. Each realization can be represented as a single point in an n-dimensional state space, while together the realizations constitute a cloud of such points. In the limit as N goes to infinity, the cloud of points can be described using the pdf

$$f(\psi) = \frac{dN}{N}, \qquad (19)$$

where dN is the number of points in a small unit volume and N is the total number of points. Statistical moments can then be calculated from either $f(\psi)$ or the ensemble representing $f(\psi)$.

Prediction of Error Statistics

A nonlinear model that contains stochastic errors can be written as the stochastic differential equation

$$d\psi = G(\psi)dt + h(\psi)dq. \qquad (20)$$

Equation (20) states that an increment in time yields an increment in ψ, which, in addition, is influenced by a random contribution from the stochastic forcing term $h(\psi)dq$, representing the model errors. The term dq describes a vector Brownian motion process with covariance $C_{qq}dt$. Since the model operator G in (20) is not an explicit function of the random variable dq, the Ito interpretation is used rather than the Stratonovich interpretation [35].

When additive Gaussian model errors forming a Markov process are used, it is possible to derive the Fokker-Planck equation (also called Kolmogorov's equation), which

describes the time evolution of the pdf $f(\psi)$ of the model state. This equation has the form

$$\frac{\partial f(\psi)}{\partial t} + \sum_i \frac{\partial(g_i f(\psi))}{\partial \psi_i} = \frac{1}{2}\sum_{i,j} \frac{\partial^2 f(\psi)(hC_{qq}h^T)_{ij}}{\partial \psi_i \partial \psi_j}, \qquad (21)$$

where g_i is the component number i of the model operator G and $hC_{qq}h^T$ is the covariance matrix for the model errors.

The Fokker-Planck equation (21) does not entail any approximations and can be considered as the fundamental equation for the time evolution of the error statistics. A detailed derivation is given in [35]. Equation (21) describes the change of the probability density in a local "volume," which depends on the divergence term describing a probability flux into the local "volume" (impact of the dynamical equation) and the diffusion term, which tends to flatten the probability density due to the effect of stochastic model errors. If (21) could be solved for the pdf, it would be possible to calculate statistical moments such as the mean and the error covariance for the model forecast to be used in the analysis scheme.

A linear model for a Gauss-Markov process, in which the initial condition is assumed to be taken from a normal distribution, has a probability density that is completely characterized by its mean and covariance for all times. We can then derive exact equations for the evolution of the mean and the covariance as a simpler alternative than solving the full Fokker-Planck equation. These moments of (21), including the error covariance (7), are easy to derive, and several methods are illustrated in [35]. The KF uses the first two moments of (21).

For a nonlinear model, the mean and covariance matrix do not in general characterize the time evolution of $f(\psi)$. These quantities do, however, determine the mean path and the width of the pdf about that path, and it is possible to solve approximate equations for the moments, which is the procedure characterizing the EKF.

The EnKF applies a Markov chain Monte Carlo (MCMC) method to solve (21). The probability density is then represented by a large ensemble of model states. By integrating these model states forward in time according to the model dynamics, as described by the stochastic differential equation (20), this ensemble prediction is equivalent to using a MCMC method to solve the Fokker-Planck equation.

Dynamical models can have stochastic terms embedded within the nonlinear model operator, and the derivation of the associated Fokker-Planck equation can become complex. Fortunately, the explicit form of the Fokker-Planck equation is not needed, since, to solve this equation using MCMC methods, it is sufficient to know that the equation and a solution exist.

Analysis Scheme

We now derive the update scheme in the KF using the ensemble covariances as defined by (17) and (18). For

convenience the time index k is omitted in the equations to follow. As shown by [9] it is essential that the observations be treated as random variables having a distribution with mean equal to the observed value and covariance equal to $C_{\epsilon\epsilon}$. Thus, we start by defining an ensemble of observations

$$d_j = d + \epsilon_j, \qquad (22)$$

where j counts from one to the number N of ensemble members. By subtracting any nonzero mean from the N samples ϵ_j, it is ensured that the simulated random measurement errors have mean equal to zero and thus the random perturbations do not introduce any bias in the update. Next we define the ensemble covariance matrix of the measurement errors as

$$C_{\epsilon\epsilon}^{e} = \overline{\epsilon \epsilon^{T}}, \qquad (23)$$

while, in the limit of infinite ensemble size this matrix converges to the prescribed error covariance matrix $C_{\epsilon\epsilon}$ used in the Kalman filter. The following discussion is valid using both an exactly prescribed $C_{\epsilon\epsilon}$ and an ensemble representation $C_{\epsilon\epsilon}^{e}$ of $C_{\epsilon\epsilon}$, which can be useful in some implementations of the analysis scheme.

The analysis step in EnKF consists of updates performed on each of the ensemble members, as given by

$$\psi_j^{a} = \psi_j^{f} + (C_{\psi\psi}^{e})^{f}M^{T}(M(C_{\psi\psi}^{e})^{f}M^{T} + C_{\epsilon\epsilon}^{e})^{-1}(d_j - M\psi_j^{f}). \quad (24)$$

With a finite ensemble size, the use of the ensemble covariances introduces an approximation of the true covariances. Furthermore, if the number of measurements is larger than the number of ensemble members, then the matrices $M(C_{\psi\psi}^{e})^{f}M^{T}$ and $C_{\epsilon\epsilon}^{e}$ are singular, and pseudo inversion must be used.

Equation (24) implies that

$$\overline{\psi^{a}} = \overline{\psi^{f}} + (C_{\psi\psi}^{e})^{f}M^{T}(M(C_{\psi\psi}^{e})^{f}M^{T} + C_{\epsilon\epsilon}^{e})^{-1}(\overline{d} - M\overline{\psi^{f}}), \quad (25)$$

where $\overline{d} = d$ since the measurement perturbations have ensemble mean equal to zero. Thus, the relation between the analyzed and predicted ensemble mean is identical to the relation between the analyzed and predicted state in the standard Kalman filter, apart from the use of $(C_{\psi\psi}^{e})^{f,a}$ and $C_{\epsilon\epsilon}^{e}$ instead of $C_{\psi\psi}^{f,a}$ and $C_{\epsilon\epsilon}$. Note that the introduction of an ensemble of observations does not affect the update of the ensemble mean.

It is now shown that, by updating each of the ensemble members using the perturbed observations, we can create a new ensemble with the correct error statistics. We derive the analyzed error covariance estimate resulting from the analysis scheme given above, although we retain the standard Kalman filter form for the analysis equations. First, (24) and (25) are used to obtain

$$\psi_j^{a} - \overline{\psi^{a}} = (I - K_{e}M)(\psi_j^{f} - \overline{\psi^{f}}) + K_{e}(d_j - \overline{d}), \qquad (26)$$

where we use the Kalman gain

$$K_{e} = (C_{\psi\psi}^{e})^{f}M^{T}(M(C_{\psi\psi}^{e})^{f}M^{T} + C_{\epsilon\epsilon}^{e})^{-1}. \qquad (27)$$

The error covariance update is then derived as

$$
\begin{aligned}
(C_{\psi\psi}^{e})^{a} &= \overline{(\psi^{a} - \overline{\psi^{a}})(\psi^{a} - \overline{\psi^{a}})^{T}} \\
&= \overline{((I - K_{e}M)(\psi^{f} - \overline{\psi^{f}}) + K_{e}(d - \overline{d}))} \\
&\quad \times \overline{((I - K_{e}M)(\psi^{f} - \overline{\psi^{f}}) + K_{e}(d - \overline{d}))^{T}} \\
&= (I - K_{e}M)\overline{(\psi^{f} - \overline{\psi^{f}})(\psi^{f} - \overline{\psi^{f}})^{T}}(I - K_{e}M)^{T} \\
&\quad + K_{e}\overline{(d - \overline{d})(d - \overline{d})^{T}}K_{e}^{T} \\
&= (I - K_{e}M)(C_{\psi\psi}^{e})^{f}(I - M^{T}K_{e}^{T}) + K_{e}C_{\epsilon\epsilon}^{e}K_{e}^{T} \\
&= (C_{\psi\psi}^{e})^{f} - K_{e}M(C_{\psi\psi}^{e})^{f} - (C_{\psi\psi}^{e})^{f}M^{T}K_{e}^{T} \\
&\quad + K_{e}(M(C_{\psi\psi}^{e})^{f}M^{T} + C_{\epsilon\epsilon}^{e})K_{e}^{T} \\
&= (I - K_{e}M)(C_{\psi\psi}^{e})^{f}. \qquad (28)
\end{aligned}
$$

The last expression in (28) is the traditional result for the minimum error covariance found in the KF analysis scheme. Thus, (28) implies that EnKF in the limit of an infinite ensemble size gives the same result as KF. It is assumed that the distributions used to generate the model-state ensemble and the observation ensemble are independent. Using a finite ensemble size, neglecting the cross-term introduces sampling errors. Note that the derivation (28) shows that the observations d must be treated as random variables to introduce the measurement error covariance matrix $C_{\epsilon\epsilon}^{e}$ into the expression. That is,

$$C_{\epsilon\epsilon}^{e} = \overline{\epsilon \epsilon^{T}} = \overline{(d - \overline{d})(d - \overline{d})^{T}}. \qquad (29)$$

A full-rank measurement error covariance matrix can be used in (27), but the use of an ensemble representation of the measurement error covariance matrix leads to an exact cancellation in the second last line in (27), which becomes

$$
\begin{aligned}
K_{e}(M(C_{\psi\psi}^{e})^{f}M^{T} + C_{\epsilon\epsilon}^{e})K_{e}^{T} &= K_{e}(M(C_{\psi\psi}^{e})^{f}M^{T} + C_{\epsilon\epsilon}^{e}) \\
&\quad \times (M(C_{\psi\psi}^{e})^{f}M^{T} + C_{\epsilon\epsilon}^{e})^{-1}M(C_{\psi\psi}^{e})^{f} \\
&= K_{e}M(C_{\psi\psi}^{e})^{f}. \qquad (30)
\end{aligned}
$$

Thus, we conclude that the use of a low-rank measurement error covariance matrix, represented by the measurement perturbations, when computing the Kalman gain, reduces the sampling errors in EnKF. The remaining sampling errors come from neglecting the cross-correlation term between the measurements and the forecast ensemble, which is nonzero with a final ensemble size, and from the approximation of the state error covariance matrix using a finite ensemble size.

The above derivation assumes that the inverse in the Kalman gain (27) exists. However, the derivation also holds when the matrix in the inversion is of low rank, for example, when the number of measurements is larger than the number of realizations and the low-rank $C_{\epsilon\epsilon}^{e}$ is used. The inverse in (27) can then be replaced with the pseudoinverse, and we can write the Kalman gain as

$$K_{e} = (C_{\psi\psi}^{e})^{f} M^{T}(M(C_{\psi\psi}^{e})^{f} M^{T} + C_{\epsilon\epsilon}^{e})^{+}. \qquad (31)$$

When the matrix in the inversion is of full rank, (31) becomes identical to (27). Using (31) the expression (30) becomes

$$
\begin{aligned}
K_{e}(M(C_{\psi\psi}^{e})^{f} M^{T} + C_{\epsilon\epsilon}^{e}) \, K_{e}^{T} &= (C_{\psi\psi}^{e})^{f} M^{T}(M(C_{\psi\psi}^{e})^{f} M^{T} + C_{\epsilon\epsilon}^{e})^{+} \\
&\quad \times (M(C_{\psi\psi}^{e})^{f} M^{T} + C_{\epsilon\epsilon}^{e}) \\
&\quad \times (M(C_{\psi\psi}^{e})^{f} M^{T} + C_{\epsilon\epsilon}^{e})^{+} M(C_{\psi\psi}^{e})^{f} \\
&= (C_{\psi\psi}^{e})^{f} M^{T}(M(C_{\psi\psi}^{e})^{f} M^{T} \\
&\quad + C_{\epsilon\epsilon}^{e})^{+} M(C_{\psi\psi}^{e})^{f} \\
&= K_{e} M(C_{\psi\psi}^{e})^{f}, \qquad (32)
\end{aligned}
$$

where we have used the property $Y^{+} = Y^{+} Y Y^{+}$ of the pseudoinverse.

It should be noted that the EnKF analysis scheme is approximate in the sense that non-Gaussian contributions in the predicted ensemble are not properly taken into account. In other words, the EnKF analysis scheme does not solve the Bayesian update equation for non-Gaussian pdfs. On the other hand, the EnKF analysis scheme is not just a resampling of a Gaussian posterior distribution. Only the updates defined by the right-hand side of (24), which are added to the prior non-Gaussian ensemble, are linear. Thus, the updated ensemble inherits many of the non-Gaussian properties from the forecast ensemble. In summary, we have a computationally efficient analysis scheme where we avoid resampling of the posterior.

Ensemble Kalman Filter with a Linear Advection Equation

The properties of EnKF are now illustrated in a simple example when used with a one-dimensional linear advection model. The model describes general transport in a prescribed background flow on a periodic domain of length 1000 m. The model has the constant advection speed $u = 1$ m/s, the grid spacing $\Delta x = 1$ m, and the time step $\Delta t = 1$ s. Given an initial condition, the solution of this model is exactly known, which facilitates realistic experiments with zero model error to examine the impact of the dynamical evolution of the error covariance.

The true initial state is sampled from a normal distribution $\mathcal{N}$, with mean equal to zero, variance equal to one, and a spatial decorrelation length of 20 m. The first guess solution is generated by drawing another sample from $\mathcal{N}$ and adding this sample to the true state. The initial ensemble of 1000 realizations is generated by adding samples drawn from $\mathcal{N}$ to the first guess solution. Thus, the initial state is assumed to have an error variance equal to one. Four measurements of the true solution, distributed regularly in the model domain, are assimilated every fifth time step. The measurements of the wave amplitude are contaminated by errors of variance equal to 0.01, in nondimensional units, and we assume uncorrelated measurement errors. The length of the integration is 300 s, which is 50 s longer than the time of 250 s needed for the solution to advect from one measurement to the next.

The example in Figure 2 illustrates the convergence of the estimated solution at various times during the experiment. In particular, Figure 2 shows how information from measurements is propagated with the advection speed and how the error variance is reduced each time measurements are assimilated. The first plot shows the result of the first update with the four measurements. Near the measurement locations, the estimated solution is consistent with both the true solution and the measurements, and the error variance is reduced accordingly. The second plot is taken at $t = 150$ s, that is, after 30 updates with measurements. Now the information from the measurements has propagated to the right with the advection speed, as seen both from direct comparison of the estimate with the true solution, as well as from the estimated variance. The final plot, which is taken at $t = 300$ s, shows that the estimate is now in good agreement with the true solution throughout the model domain. Note also the linear increase in error variance to the right of the measurements, which is caused by the addition of model errors at each time step. It is also clear that the estimated solution deteriorates far from the measurements in the advection direction. For linear models with regular measurements at fixed locations and stationary error statistics, the increase of error variance from model errors balances the reduction from the updates with measurements.

Discussion

We now have a complete system of equations that constitute the EnKF, and the similarity with the standard KF is maintained both for the prediction of error covariances

and in the analysis scheme. For linear dynamics the EnKF solution converges exactly to the KF solution with increasing ensemble size.

One of the advantages of EnKF is that, for nonlinear models, the equation for the mean is solved and no closure assumption is used since each ensemble member is integrated by the full nonlinear model. This nonlinear error evolution is contrary to the approximate equation for the mean (16), which is used in EKF.

Thus, it is possible to interpret EnKF as a purely statistical Monte Carlo method where the ensemble of model states evolves in state space with the mean as the best estimate and the spreading of the ensemble as the error variance. At measurement times each observation is represented by another ensemble, where the mean is the actual measurement and the variance of the ensemble represents the measurement errors. Thus, we combine a stochastic prediction step with a stochastic analysis step.

PROBABILISTIC FORMULATION

For the ensemble Kalman smoother (EnKS) [8], the estimate at a particular time is updated based on past, present, and future measurements. In contrast, a filter estimate is influenced only by the past and present measurements. Thus, EnKF becomes a special case of EnKS, where information from measurements is not projected backward in time. The assumptions of measurement errors being independent in time and the dynamical model being a Markov process are sufficient to derive the EnKF and the EnKS. These assumptions are normally not critical and are already used in the original KF. It is also possible to include the estimation of static model parameters in a consistent manner. The combined parameter and state estimation problem for a dynamical model can be formulated as finding the joint pdf of the parameters and model state, given a set of measurements and a dynamical model with known uncertainties.

Model Equations and Measurements

We consider a model with associated initial and boundary conditions on the spatial domain $\mathcal{D}$ with boundary $\partial\mathcal{D}$, and with observations
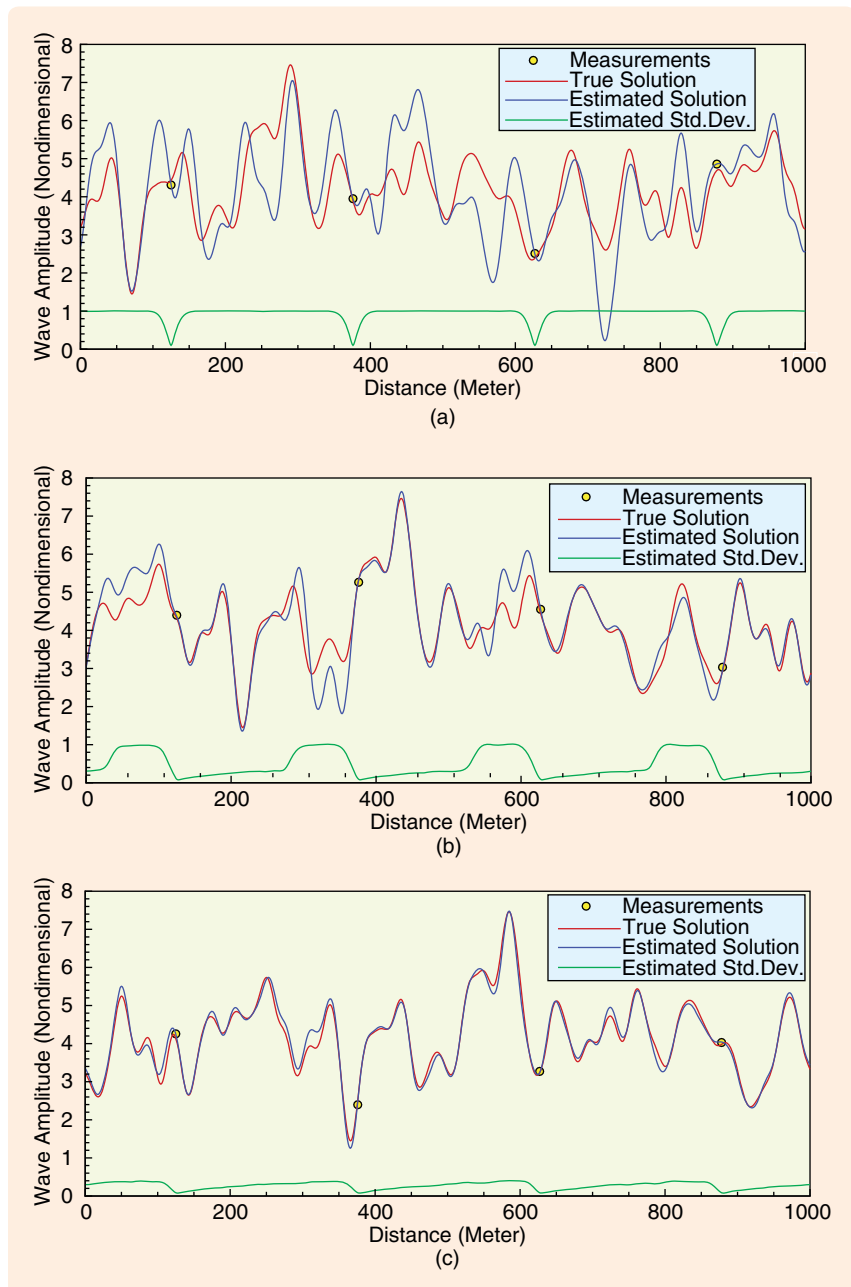

FIGURE 2 An ensemble Kalman filter experiment. For this experiment a linear advection equation illustrates how a limited ensemble size of 100 realizations facilitates estimation in a high-dimensional system whose state vector contains 1000 entries. The plots show the reference solution, measurements, estimate, and standard deviation at three different times, (a) $t = 5$ s, (b) $t = 150$ s, and (c) $t = 300$ s.

$$\frac{\partial\psi(x,t)}{\partial t} = G(\psi(x,t), \alpha(x)) + q(x,t), \tag{33}$$

$$\psi(x, t_0) = \Psi_0(x) + a(x), \tag{34}$$

$$\psi(\xi, t) = \Psi_b(\xi, t) + b(\xi, t), \text{ for all } \xi \in \delta\mathcal{D}, \tag{35}$$

$$\alpha(x) = \alpha_0(x) + \alpha'(x), \tag{36}$$

$$\mathcal{M}[\psi, \alpha] = d + \epsilon. \tag{37}$$

The model state $\psi(x, t) \in \mathcal{R}^{n_\psi}$ is a vector consisting of the n_ψ model variables, where each variable is a function of
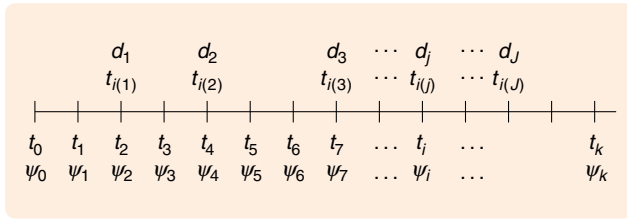
FIGURE 3 Discretization in time. The time interval is discretized into $k + 1$ nodes, t_0 to t_k, where the model state vector $\psi_i = \psi(t_i)$ is defined. The measurement vectors d_j are available at the discrete subset of times $t_{i(j)}$, where $j = 1, \ldots, j$.

space and time. The nonlinear model is defined by (33), where $G(\psi, \alpha) \in \mathcal{R}^{n_\psi}$ is the nonlinear model operator. More general forms can be used for the nonlinear model operator, although (33) suffices to demonstrate the methods considered here.

The model state is assumed to evolve in time from the initial state $\Psi_0(x) \in \mathcal{R}^{n_\psi}$ defined in (34), under the constraints of the boundary conditions $\Psi_b(\xi, t) \in \mathcal{R}^{n_\psi}$ defined in (35). The coordinate ξ runs over the surface $\partial \mathcal{D}$, where the boundary conditions are defined. The variable b is used to represent errors in the boundary conditions.

We define $\alpha(x) \in \mathcal{R}^{n_\alpha}$ as the set of n_α poorly known parameters of the model. The parameters can be a vector of spatial fields in the form written here, or, alternatively, a vector of scalars, and are assumed to be constant in time. A prior estimate $\alpha_0(x) \in \mathcal{R}^{n_\alpha}$ of the vector of parameters $\alpha(x) \in \mathcal{R}^{n_\alpha}$ is introduced through (36), and possible errors in the prior are represented by $\alpha'(x)$.

Additional conditions are present in the form of the measurements $d \in \mathcal{R}^M$. Both direct point measurements of the model solution and more complex parameters that are nonlinearly related to the model state can be used. For the time being we restrict ourselves to the case of linear measurements. An example of a direct measurement functional is then

$$\mathcal{M}_i[\psi] = \int\int \psi^\mathsf{T}(x, t)\delta_{\psi_i}\delta(t - t_i)\delta(x - x_i)dt\,dx = \psi(x_i, t_i)\delta_{\psi_i},$$
(38)

where the integration is over the space and time domain of the model. The measurement d_i is related to the model-state variable as selected by the vector $\delta_{\psi_i} \in \mathcal{R}^{n_\psi}$ and evaluated at the space and time location (x_i, t_i). If a model with three state variables is used and the second variable is measured, then δ_{ψ_i} becomes the vector $(0, 1, 0)^\mathsf{T}$, while $\delta(t - t_i)$ and $\delta(x - x_i)$ are Dirac delta functions.

In (33)–(37) we include unknown error terms, q, a, b, α', and ϵ, which represent errors in the model equations, the initial and boundary conditions, the first guess for the model parameters, and the measurements, respectively. Without these error terms the system as given above is overdetermined and has no solution. On the other hand,

when we introduce these error terms without additional conditions, the system has infinitely many solutions. The way to proceed is to introduce a statistical hypothesis about the errors, for example, assuming that the errors are normally distributed with means equal to zero and known error covariances.

Bayes Theorem

We now consider the model variables, the poorly known parameters, the initial and boundary conditions, and the measurements as random variables, which can be described by pdfs. The joint pdf for the model state, as a function of space, time, and the parameters, is $f(\psi, \alpha)$. Furthermore, for the measurements we can define the likelihood function $f(d\,|\,\psi, \alpha)$. Thus, we may have measurements of both the model state and the parameters. Using Bayes theorem, the parameter and state estimation problem is now written in the simplified form

$$f(\psi, \alpha\,|\,d) = \gamma f(\psi, \alpha)f(d\,|\,\psi, \alpha),$$
(39)

where γ is a constant of proportionality whose computation requires the evaluation of the integral of (39) over the high-dimensional solution and parameter space.

Parameter estimation problems, in particular, for applications involving high-dimensional models, such as oceanic, atmospheric, marine ecosystem, hydrology, and petroleum applications, often do not include the model state as a variable to be estimated. It is more common to first solve for the poorly known parameters by minimizing an appropriate cost function where the model equations act as a strong constraint and then rerun the model to find the model solution. It is then implicitly assumed that the model does not contain errors, an assumption that generally is invalid.

In the dynamical model, we specify initial and boundary conditions as random variables, and we include prior information about the parameters. Thus, we define the pdfs $f(\psi_0)$, $f(\psi_b)$, and $f(\alpha)$ for the estimates ψ_0, ψ_b, and α of the initial and boundary conditions, and the parameters, respectively. Instead of $f(\psi, \alpha)$, we write

$$f(\psi, \alpha, \psi_0, \psi_b) = f(\psi\,|\,\alpha, \psi_0, \psi_b)f(\psi_0)f(\psi_b)f(\alpha).$$
(40)

Equation (39) should accordingly be written as

$$f(\psi, \alpha, \psi_0, \psi_b\,|\,d) = \gamma f(\psi\,|\,\alpha, \psi_0, \psi_b)f(\psi_0)f(\psi_b)f(\alpha)f(d\,|\,\psi, \alpha),$$
(41)

where it is also assumed that the boundary conditions and initial conditions are independent, although this assumption may not be true for the locations where initial and boundary conditions intersect at t_0. Here the pdf $f(\psi\,|\,\alpha, \psi_0, \psi_b)$ is the prior density for the model solution given the parameters and initial and boundary conditions.

Discrete Formulation

In the following discussion we work with a model state that is discretized in time, that is, $\psi(x, t)$ is represented at fixed time intervals as $\psi_i(x) = \psi(x, t_i)$ with $i = 0, 1, \ldots, k$; see Figure 3. Furthermore, we define the pdf for the model integration from time t_{i-1} to t_i as $f(\psi_i | \psi_{i-1}, \alpha, \psi_b(t_i))$, which assumes that the model is a first-order Markov process. The joint pdf for the model solution and the parameters in (40) can now be written as

$$
\begin{aligned}
f(\psi_1, \ldots, \psi_k, \alpha, \psi_0, \psi_b) \\
= f(\alpha)f(\psi_b)f(\psi_0)\prod_{i=1}^{k} f(\psi_i | \psi_{i-1}, \alpha, \psi_b).
\end{aligned}
\tag{42}
$$

Independent Measurements

We now assume that the measurements $d \in \mathcal{R}^M$ can be divided into subsets of measurement vectors $d_j \in \mathcal{R}^{m_j}$, collected at times $t_{i(j)}$, with $j = 1, \ldots, J$ and $0 < i(1) < i(2) < \cdots < i(J) < k$. The subset d_j depends only on $\psi(t_{i(j)}) = \psi_{i(j)}$ and α. Furthermore, it is assumed that the measurement errors are uncorrelated in time. We can then write

$$
f(d | \psi, \alpha) = \prod_{j=1}^{J} f(d_j | \psi_{i(j)}, \alpha),
\tag{43}
$$

and from Bayes theorem we obtain

$$
\begin{aligned}
f(\psi_1, \ldots, \psi_k, \alpha, \psi_0, \psi_b | d) \\
= \gamma f(\alpha)f(\psi_0)f(\psi_b)\prod_{i=1}^{k} f(\psi_i | \psi_{i-1}, \alpha)\prod_{j=1}^{J} f(d_j | \psi_{i(j)}, \alpha).
\end{aligned}
\tag{44}
$$

Sequential Processing of Measurements

It is shown in [36] and [37] that, in the case of time-correlated model errors, it is possible to reformulate the problem as a first-order Markov process by augmenting the model errors to the model-state vector. A simple equation forced by white noise can be used to simulate the time evolution of the model errors.

In [38] it is shown that a general smoother and filter can be derived from the Bayesian formulation given in (44). We now rewrite (44) as a sequence of iterations

$$
\begin{aligned}
f(\psi_1, \ldots, \psi_{i(j)}, \alpha, \psi_0, \psi_b | d_1, \ldots, d_j) \\
= \gamma f(\psi_1, \ldots, \psi_{i(j-1)}, \alpha, \psi_0, \psi_b | d_1, \ldots, d_{j-1}) \\
\times \prod_{i=i(j-1)+1}^{i(j)} f(\psi_i | \psi_{i-1}, \alpha)f(d_j | \psi_{i(j)}, \alpha).
\end{aligned}
\tag{45}
$$

Thus, we formulate the combined parameter and state-estimation problem using Bayesian statistics and see that, under the condition that measurement errors are independent in time and the dynamical model is a Markov process, a recursive formulation can be used for Bayes theorem.

That is, the model state and parameters with their respective uncertainties are updated sequentially in time whenever the measurements become available.

We note again that this recursion does not introduce any significant approximations and thus describes the full inverse problem as long as the model is a Markov process and the measurements errors are independent in time. Further, for many problems the recursive processing of measurements provides a better posed approach for solving the inverse problem than trying to process all of the measurements simultaneously as is normally done in variational formulations. Sequential processing is also convenient for forecasting problems where new measurements can be processed when they arrive without recomputing the full inversion.

Ensemble Smoother

The ensemble smoother (ES) can be derived by assuming that the pdfs for the model prediction as well as the likelihood are Gaussian and by using the original Bayes theorem (41). The derivation requires that we approximate the pdfs resulting from an integration of the ensemble through the whole assimilation time period with Gaussian pdfs. We can then replace Bayes theorem with a least squares cost function similar to (1), but with the time dimension included, and the analysis becomes a standard variance minimizing analysis in space and time. All of the data are processed in one step, and the solution is updated as a function of space and time, using the space-time covariances estimated from the ensemble of model realizations. The ES in [39] is computed as a first-guess estimate, which is the mean of the freely evolving ensemble, plus a linear combination of time-dependent influence functions, which are calculated from the ensemble statistics. Thus, the method is equivalent to a variance-minimizing objective analysis method where the time dimension is included.

Ensemble Kalman Smoother

An assumption of Gaussian pdfs for the model prediction (the prior) and the distribution for the data (the likelihood function) in (45) allows us to replace the Bayesian update formula with a least squares cost function similar to (1) but additionally including the state vector at all previous times. Again the cost function is minimized using a standard variance-minimizing analysis scheme, involving a state variable defined from the initial time to the current update time. That is, we also update the state variables backward in time using the combined time and space ensemble covariances. This scheme results in the EnKS as in [38].

Ensemble Kalman Filter

The EnKF is just a special case of EnKS where the updates at previous times are skipped. EnKF is obtained by
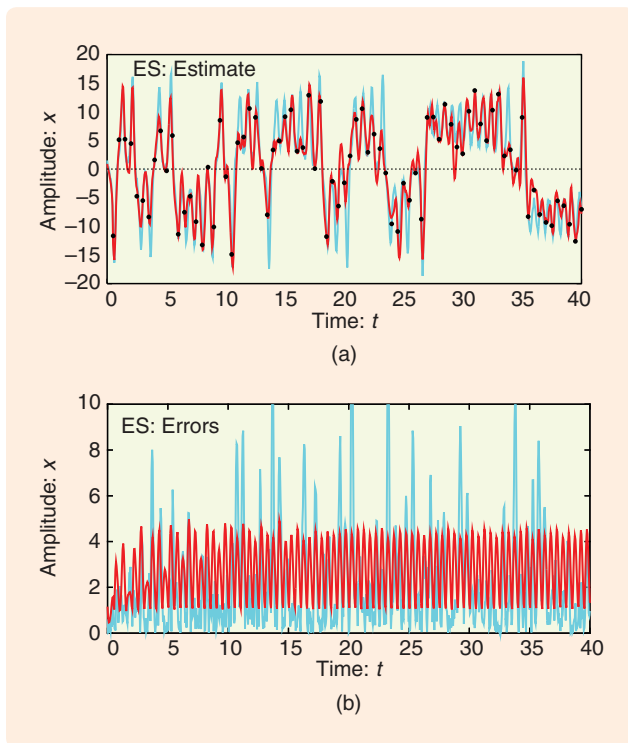
FIGURE 4 Ensemble smoother. (a) shows the inverse estimate (red line) and reference solution (blue line) for *x*. (b) shows the corresponding estimated standard deviations (red line) as well as the absolute value of the difference between the reference solution and the estimate, that is, the real posterior errors (blue line). (Reproduced from [38] with permission.)

integrating out the state variables at all previous times from (45) and assuming that the resulting model pdf for the current time as well as the likelihood function are Gaussian. The incremental update (45) can then be replaced by the penalty function (1), leading to the standard Kalman filter analysis equations. Thus, the measurements are filtered. At the final time, or, actually, from the latest update and for predictions into the future, EnKF and EnKS provide identical solutions.

EXAMPLE WITH THE LORENZ EQUATIONS

The example from [40] and [38] with the chaotic Lorenz model of [41] is now used to compare ES, EnKS, and EnKF. The Lorenz model consists of the coupled system of nonlinear ordinary differential equations given by

$$\frac{dx}{dt} = \gamma(y - x), \tag{46}$$

$$\frac{dy}{dt} = \rho x - y - xz, \tag{47}$$

$$\frac{dz}{dt} = xy - \beta z. \tag{48}$$

Here $x(t)$, $y(t)$, and $z(t)$ are the dependent variables, and we choose the parameter values $\gamma = 10$, $\rho = 28$, and $\beta = 8/3$. The initial conditions for the reference case are

given by $(x_0, y_0, z_0) = (1.508870, -1.531271, 25.46091)$ and the time interval is $t \in [0, 40]$.

The observations and initial conditions are simulated by adding normally distributed white noise with zero mean and variance equal to 2.0 to the reference solution. All of the variables x, y, and z are measured. In the calculation of the ensemble statistics, an ensemble of 1000 members is used. The same simulation is rerun with various ensemble sizes, and the differences between the results are negligible with as few as 50 ensemble members.

The three methods discussed above are now examined and compared in an experiment where the time between measurements is $\Delta t_{obs} = 0.5$, which is similar to Experiment B in [40]. In the upper plots in figures 4–6, the red line denotes the estimate and the blue line is the reference solution. In the lower plots the red line is the standard deviation estimated from ensemble statistics, while the blue line is the true residuals with respect to the reference solution.

Ensemble Smoother Solution

The ES solution for the x-component and the associated estimated error variance are given in Figure 4. It is found that the ES performs rather poorly with the current data density. Note, however, that even if the fit to the reference trajectory is poor, the ES solution captures most of the transitions. The main problem is related to the estimate of the amplitudes in the reference solution. The problem is linked to the appearance of non-Gaussian contributions in the distribution for the model evolution, which can be expected in such a strongly nonlinear case.

Clearly, the error estimates evaluated from the posterior ensemble are not large enough at the peaks where the smoother performs poorly. The underestimated errors again result from neglecting the non-Gaussian contribution from the probability distribution for the model evolution. Otherwise, the error estimate looks reasonable with minima at the measurement locations and maxima between the measurements. Note again that if a linear model is used, then the posterior density becomes Gaussian and the ES provides, in the limit of an infinite ensemble size, the same solution as the EnKS and the Kalman smoother.

Ensemble Kalman Filter Solution

EnKF does a reasonably good job tracking the reference solution with the lower data density, as can be seen in Figure 5. One transition is missed near $t = 18$, while EnKF has problems, for example, at $t = 1$, 5, 9, 10, 13, 17, 19, 23, 26, and 34. The error variance estimate is consistent, showing large peaks at the locations where the estimate obviously has problems tracking the reference solution. Note also the similarity between the absolute value of the residual between the reference solution and the estimate, and the estimated standard deviation. For all peaks in the residual, a corresponding peak is present in the error variance estimate.

The error estimates show the same behavior as in [32] with very strong error growth when the model solution passes through the unstable regions of the state space and otherwise weak error variance growth or even decay in the stable regions. Note, for example, the low error variance for $t \in [28, 34]$ corresponding to the oscillation of the solution around one of the attractors.

In this case, the nonlinearity of the problem causes EnKF to perform better than the ES. In fact, at each update, the realizations are pulled toward the true solution and are not allowed to diverge toward the wrong attractors of the system. In addition, the Gaussian increments of the ensemble members lead to an approximately Gaussian ensemble distributed around the true solution. This property of the sequential updating is not exploited in the ES, where realizations evolve freely and lead to non-Gaussian ensemble distributions. Note again that if the model dynamics are linear, then, in the limit of an infinite ensemble size, EnKF gives the same solution as the Kalman filter and the ES solution gives a better result than EnKF.

Ensemble Kalman Smoother Solution
Figure 6 shows the solution obtained by EnKS. This solution is smoother in time than the EnKF solution and provides a better fit to the reference trajectory. All of the problematic locations in the EnKF solution are recovered in the smoother estimate. Note, for example, that the additional transitions at $t = 1$, 5, 13, and 34 in the EnKF solution are eliminated in the smoother. In addition, the missed transition at $t = 17$ is recovered by EnKS.

The error estimates are reduced throughout the time interval. In particular the large peaks in the EnKF solution are now significantly reduced. As for the EnKF solution, there are corresponding peaks in the error estimates for all the peaks in the residuals, which suggests that the EnKS error estimate is consistent with the true errors. In fact, in [40], it is found that the EnKS solution with $\Delta t_{\text{obs}} = 0.5$ seems to do as well or better than the EnKF solution with $\Delta t_{\text{obs}} = 0.25$.

Note that, if only z is measured in the Lorenz equations, the measured information is not sufficient to determine the solution. EnKF in this case develops realizations located at both attractors, and a bimodal distribution develops. The EnKF update breaks down with the bimodal distribution, but even the use of a Bayesian update in a particle filter does not suffice to determine the correct solution in this case since the bimodal distribution has the same probability for both peaks of the distribution. Note also that the assumption of Gaussian pdfs in the analysis equation is an approximation, whose severity must be judged on a case-by-case basis.

PRACTICAL IMPLEMENTATION
In [37] it is shown that the EnKF analysis scheme can be formulated in terms of the ensemble without reference to the ensemble covariance matrix, which allows for efficient numerical implementation and an alternative interpretation of the method. In the discussion below, we omit the time index, since all variables refer to the same update time.

Ensemble Representation of the Covariance
We define the matrix A whose columns are the ensemble members $\psi_i \in \mathcal{R}^n$ by

$$A = (\psi_1, \psi_2, \ldots, \psi_N) \in \mathcal{R}^{n \times N}, \qquad (49)$$

where N is the number of ensemble members and n is the size of the model state vector. The ensemble mean is stored in each column of $\overline{A}$, which is defined as

$$\overline{A} = A\mathbf{1}_N, \qquad (50)$$

where $\mathbf{1}_N \in \mathcal{R}^{N \times N}$ is the matrix whose entries are all equal $1/N$. We then define the ensemble perturbation matrix as

$$A' = A - \overline{A} = A(I - \mathbf{1}_N). \qquad (51)$$

The ensemble covariance matrix $C_{\psi\psi}^e \in \mathcal{R}^{n \times n}$ can be defined as

$$C_{\psi\psi}^e = \frac{1}{N-1} A'(A')^{\mathrm{T}}. \qquad (52)$$

Measurement Perturbations
Given a vector of measurements $d \in \mathcal{R}^m$, where m is the number of measurements, we define the N vectors of perturbed observations as

$$d_j = d + \epsilon_j, \; j = 1, \ldots, N, \qquad (53)$$

which are stored in the columns of the matrix

$$D = (d_1, d_2, \ldots, d_N) \in \mathcal{R}^{m \times N}, \qquad (54)$$

while the ensemble of perturbations, with ensemble mean equal to zero, are stored in the matrix

$$E = (\epsilon_1, \epsilon_2, \ldots, \epsilon_N) \in \mathcal{R}^{m \times N}, \qquad (55)$$

from which we construct the ensemble representation of the measurement error covariance matrix

$$C_{\epsilon\epsilon}^e = \frac{1}{N-1} EE^{\mathrm{T}}. \qquad (56)$$

Analysis Equation
The analysis equation (24), expressed in terms of the ensemble matrices, is

$$A^{\mathrm{a}} = A + C_{\psi\psi}^e M^{\mathrm{T}} (MC_{\psi\psi}^e M^{\mathrm{T}} + C_{\epsilon\epsilon}^e)^{-1}(d - MA). \qquad (57)$$
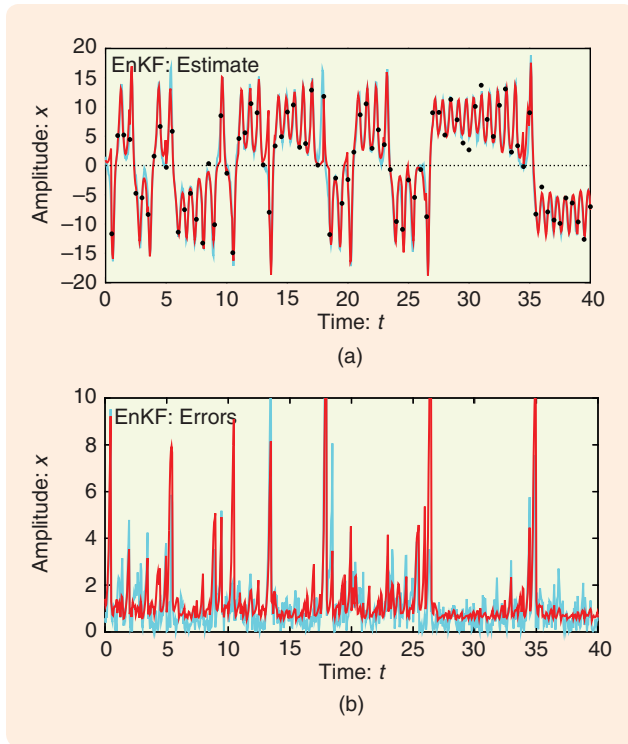
FIGURE 5 Ensemble Kalman filter. (a) shows the inverse estimate (red line) and reference solution (blue line) for x. (b) shows the corresponding estimated standard deviations (red line) as well as the absolute value of the difference between the reference solution and the estimate, that is, the real posterior errors (blue line). (Reproduced from [38] with permission.)

Using the ensemble of innovation vectors defined as

$$D' = D - MA, \tag{58}$$

along with the definitions of the ensemble error covariance matrices in (52) and (56), the analysis can be expressed as

$$A^a = A + A'A'^T M^T (MA'A'^T M^T + EE^T)^{-1}D', \tag{59}$$

where all references to the error covariance matrices are eliminated.

We now introduce the matrix $S \in \mathcal{R}^{m \times N}$ holding the measurements of the ensemble perturbations by

$$S = MA', \tag{60}$$

and the matrix $C \in \mathcal{R}^{m \times m}$,

$$C = SS^T + (N-1)C_{\epsilon\epsilon}. \tag{61}$$

Here we can use the full-rank, exact measurement error covariance matrix $C_{\epsilon\epsilon}$ as well as the low-rank representation $C^e_{\epsilon\epsilon}$ defined in (56).

The analysis equation (59) can then be written as

$$
\begin{aligned}
A^a &= A + A'S^T C^{-1} D' \\
&= A + A(I - \mathbf{1}_N)S^T C^{-1} D' \\
&= A(I + (I - \mathbf{1}_N)S^T C^{-1} D') \\
&= A(I + S^T C^{-1} D') \\
&= AX,
\end{aligned} \tag{62}
$$

where we use (51) and $\mathbf{1}_N S^T \equiv \mathbf{0}$. The matrix $X \in \mathcal{R}^{N \times N}$ is defined as

$$X = I + S^T C^{-1} D'. \tag{63}$$

Thus, the EnKF analysis becomes a combination of the forecast ensemble members and is searched for in the space spanned by the forecast ensemble.

It is clear that (62) is a stochastic scheme due to the use of randomly perturbed measurements. Thus, (62) allows for a nice interpretation of EnKF as a sequential Markov chain Monte Carlo algorithm, while making it easy to understand and implement the method. The efficient and stable numerical implementation of the analysis scheme is discussed in [8], including the case in which C is singular due to the number of measurements being larger than the number of realizations.

In practice, the ensemble size is critical since the computational cost scales linearly with the number of realizations. That is, each individual realization needs to be integrated forward in time. The cost associated with the ensemble integration motivates the use of an ensemble with the minimum number of realizations that can provide acceptable accuracy.

There are two major sources of sampling errors in EnKF, namely, the use of a finite ensemble of stochastic model realizations as well as the introduction of stochastic measurement perturbations [8], [42]. In addition, stochastic model errors influence the predicted error statistics, which is approximated by the ensemble. The sampling of physically acceptable model realizations and realizations of model errors is chosen to ensure that the ensemble matrix has full rank and good conditioning. Furthermore, stochastic perturbation of measurements used in EnKF can be avoided using a square root implementation of the analysis scheme, to be discussed below.

EnKF for Combined Parameter and State Estimation
When using EnKF to estimate poorly known model parameters, we start by representing the prior pdfs of the parameters by an ensemble of realizations, which is augmented to the state ensemble matrix A at the update steps. The poorly known parameters are then updated using the variance-minimizing analysis scheme, where the covariances between the predicted data and the parameters are used to update the parameters.

The updated ensemble for the parameters is included in the space defined by the initial ensemble of realizations. Thus, EnKF reduces the dimension of the combined parameter and state estimation problem to a size given by the dimension of the ensemble space. This simplification allows us to handle large sets of parameters, but it requires that the true parameters can be well represented in the ensemble space.

The parameter estimation approach used in EnKF and EnKS is a statistical minimization, or sampling of a posterior pdf, rather than a traditional minimization of a cost function. Thus, EnKF does not to the same extent suffer from the typical problems of converging to local minima as in parameter-estimation methods. EnKF rather has a problem with multimodal pdfs. However, the EnKF does not search for the mode but rather the mean of the distribution. Thus, in many cases where a minimization method might converge to a local minimum, EnKF provides an estimate that is the mean of the posterior. An important point is that the sequential updating used in EnKF reduces the risk of development of multimodal distributions, a result that is supported by the Lorenz example.

DETERMINISTIC SQUARE ROOT SCHEME

The perturbation of measurements used in the EnKF standard analysis equation (57) is an additional source of sampling error. However, methods such as the square root scheme compute the analysis without perturbing the measurements [10]–[13], [43], [44].

Based on results from [10]–[13], a variant of the square root analysis scheme is derived in [42] and further elaborated on in [8]. The perturbation of measurements is avoided, and the scheme solves for the analysis without imposing any additional approximations, such as the assumption of uncorrelated measurement errors or knowledge of the inverse of the measurement error covariance matrix. This implementation requires the inverse of the matrix C, defined in (61), which can be computed efficiently, either using the low-rank ensemble representation C_e or by projecting the measurement error covariance matrix onto the space defined by the columns in S from (60). This version of the square root scheme is now presented.

Updating the Mean

In the square root scheme, the analyzed ensemble mean is computed from the standard Kalman filter analysis equation, which can be obtained by multiplying the first line in (62) from the right with $\mathbf{1}_N$, so that each column in the resulting equation for the mean becomes

$$\overline{\psi}^{a} = \overline{\psi}^{f} + A' S^{T} C^{-1}(d - M\overline{\psi}^{f}). \tag{64}$$

Updating the Ensemble Perturbations

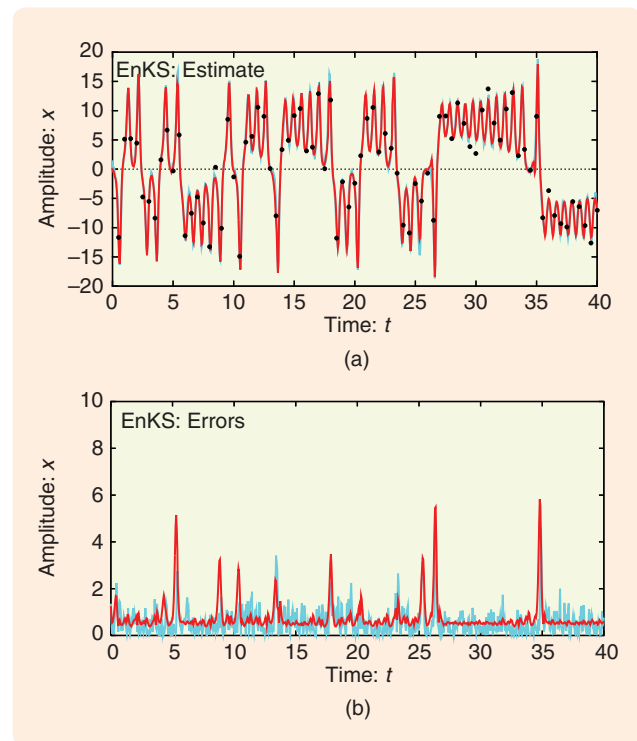The deterministic algorithm used to update the ensemble perturbations is derived starting from the traditional

FIGURE 6 Ensemble Kalman smoother. (a) shows the inverse estimate (red line) and reference solution (blue line) for x. (b) shows the corresponding estimated standard deviations (red line) as well as the absolute value of the difference between the reference solution and the estimate, that is, the real posterior errors (blue line). (Reproduced from [38] with permission.)

analysis equation for the covariance update (28) in the Kalman filter. By using the ensemble covariances, (28) can be written as

$$(C_{\psi\psi}^{e})^{a}$$
$$= (C_{\psi\psi}^{e})^{f} - (C_{\psi\psi}^{e})^{f} M^{T}(M(C_{\psi\psi}^{e})^{f} M^{T} + R)^{-1} M(C_{\psi\psi}^{e})^{f}, \tag{65}$$

with the time index dropped for convenience. When using the ensemble representation for the error covariance matrix $C_{\epsilon\epsilon}^{e}$ defined in (52), (65) becomes

$$A^{a'} A^{a'T} = A'(I - S^{T} C^{-1} S) A^{T}, \tag{66}$$

where S and C are defined in (60) and (61), and we drop the superscripts "f" on the forecast ensemble. We now derive an equation for updating the ensemble perturbations A' by defining a factorization of (66), which does not involve the measurements or measurement perturbations.

We start by forming C as defined in (61). For now we assume that C^{-1} exists, which requires that the rank of the ensemble be greater than the number of measurements. The low-rank case involves pseudo inversion [8]. Note also that the use of a full rank $C_{\epsilon\epsilon}^{e}$ can result in a full rank C even when $m \geq N$.

By computing the eigenvalue decomposition $Z\Lambda Z^T = C$, we obtain the inverse of C as

$$C^{-1} = Z\Lambda^{-1}Z^T, \qquad (67)$$

where $Z \in \mathcal{R}^{m \times m}$ is an orthogonal matrix and $\Lambda \in \mathcal{R}^{m \times m}$ is diagonal. The eigenvalue decomposition may be the most demanding computation required for the analysis when m is large. An efficient alternative inversion algorithm is presented in [8].

We now write (66) as

$$\begin{aligned} A^{a'}A^{a'T} &= A'(I - S^T Z\Lambda^{-1}Z^T S)A'^T \\ &= A'(I - (\Lambda^{-1/2}Z^T S)^T(\Lambda^{-1/2}Z^T S))A'^T \\ &= A'(I - X_2^T X_2)A'^T, \qquad (68) \end{aligned}$$

where $X_2 \in \mathcal{R}^{m \times N}$ is defined as

$$X_2 = \Lambda^{-1/2}Z^T S, \qquad (69)$$

and where rank $(X_2) = \min(m, N{-}1)$. Thus, X_2 is a projection of S onto the eigenvectors of C scaled by the square root of the eigenvalues of C.

Next we compute the singular value decomposition of X_2 given by

$$U_2 \Sigma_2 V_2^T = X_2, \qquad (70)$$

with $U_2 \in \mathcal{R}^{m \times m}$, $\Sigma_2 \in \mathcal{R}^{m \times N}$ and $V_2 \in \mathcal{R}^{N \times N}$. Since U_2 and V_2 are orthogonal matrices, (68) can be written

$$\begin{aligned} A^{a'}A^{a'T} &= A'(I - [U_2\Sigma_2 V_2^T]^T[U_2\Sigma_2 V_2^T])A'^T \\ &= A'(I - V_2\Sigma_2^T\Sigma_2 V_2^T)A'^T \\ &= A'V_2(I - \Sigma_2^T\Sigma_2)V_2^T A'^T \\ &= (A'V_2\sqrt{I - \Sigma_2^T\Sigma_2})(A'V_2\sqrt{I - \Sigma_2^T\Sigma_2})^T. \qquad (71) \end{aligned}$$

Thus, a solution for the analysis ensemble perturbations is

$$A^{a'} = A'V_2\sqrt{I - \Sigma_2^T\Sigma_2}. \qquad (72)$$

As noted in [45] the update equation (72) does not conserve the mean of the ensemble perturbations and in fact leads to the production of outliers that contain most of the ensemble variance as explained in [46] and [8], which is further illustrated in the example below.

We now write the square root update in the more general form

$$A^{a'} = A'T, \qquad (73)$$

where T is a square root transformation matrix.

It is shown in [44] and [47] that for the square root analysis scheme to be unbiased and preserve the zero mean in the updated perturbations, the vector $(1/N)\mathbf{1}$, where $\mathbf{1} \in \mathcal{R}^N$ has all components equal to one, must be an eigenvector of the square root transformation matrix T. As noted in [44] and [47], this condition is not satisfied for the update in (72).

Multiplying (73) from the right with the vector $\mathbf{1}$ and assuming that $(1/N)\mathbf{1}$ is an eigenvector of T, we can write

$$\mathbf{0} = A^{a'}\mathbf{1} = A'T\mathbf{1} = \lambda A'\mathbf{1} = \mathbf{0}. \qquad (74)$$

Equation (74) shows that a sufficient condition for the mean to be unbiased is that $(1/N)\mathbf{1}$ be an eigenvector of T. If the transform matrix is of full rank, then this condition is also necessary [47].

The symmetric square root solution for the analysis ensemble perturbations is defined as

$$A^{a'} = A'V_2(I - \Sigma_2^T\Sigma_2)^{1/2}V_2^T. \qquad (75)$$

It is easy to show that (75) is also a factorization of (71) since V_2 is an orthogonal matrix. As shown in [44], [47], the symmetric square root has an eigenvector equal to $(1/N)\mathbf{1}$ and is unbiased. In addition, the symmetric square root resolves the issue with outliers in the factorization used in (72). The analysis update of the perturbations becomes a symmetric contraction of the forecast ensemble perturbations. Thus, if the predicted ensemble members have a non-Gaussian distribution, then the updated distribution retains the shape but the variance is reduced.

A randomization of the analysis update can be used to generate updated perturbations that better resemble a Gaussian distribution [42]. Thus, we write the symmetric square root solution (75) as

$$A^{a'} = A'V_2(I - \Sigma_2^T\Sigma_2)^{1/2}V_2^T\Phi^T, \qquad (76)$$

where Φ is a mean-preserving random orthogonal matrix, which can be computed using the algorithm from [44].

The properties of the square root schemes are illustrated in Figure 7, which shows the resulting ensemble updates using several variants of the EnKF analysis scheme. The Lorenz equations (46)–(48) are used since the strong nonlinearities lead to the development of a non-Gaussian distribution for the forecast ensemble. Three observations are used in the update step. Each ensemble member is plotted as a circle in the x, y plane. In Figure 7(a) and (b) the forecast ensemble members are plotted as the blue circles, which have a non-Gaussian distribution in the x, y plane.

In Figure 7(a) the updated analysis from the "one-sided" square root scheme in (72) is shown as the yellow circles. It can be seen that $N - 3$ of the updated ensemble perturbations collapse onto $(0, 0)$, while the three non-zero "outliers," one for each measurement, determine the ensemble variance. However, one of the outliers is

too close to zero to be distinguished from the other points at zero. The variance of the updated ensemble is correct, but the analysis introduces a bias through a shift in the ensemble mean. The shift in the mean should come as no surprise since we do not impose a condition for the conservation of the mean when the update equation is derived. The particular ensemble collapse related to the use of (72) is discussed and explained in [8]. It is in fact shown that with three measurements and a diagonal measurement error covariance matrix, we obtain an ensemble with three outliers, while the remainder of the perturbations collapse onto zero.

In Figure 7(a) the updated analysis from the symmetric square root scheme in (75) is shown as the red circles. This scheme has the property that it rescales the ensemble of perturbations without changing the original shape of the perturbations. Thus, the scheme allows for preserving possible non-Gaussian structures in the ensemble during the update. We also note that the symmetric square root scheme from (75) is unbiased and thus preserves the mean [44].

In Figure 7(b) the updated analysis from the symmetric square root scheme from (76), which includes an additional mean-preserving random rotation, is plotted using the green circles. It is clear that the ensemble of updated perturbations now has a Gaussian shape, and the non-Gaussian shape of the forecast ensemble perturbations is lost. The random rotation completely destroys any prior structure in the ensemble by randomly redistributing the variability among all of the ensemble members. Thus, the random rotation acts as a complete resampling from a Gaussian distribution, while preserving the ensemble mean and variance.

Figure 7(b) also shows the updated analysis from the standard EnKF scheme from (62), where the measurements are randomly perturbed to represent their uncertainty. The standard EnKF analysis becomes similar to the symmetric square root analysis with random rotation. As with the symmetric square root analysis, most of the non-Gaussian shape of the forecast ensemble is lost. However, only the increment in the standard EnKF analysis is
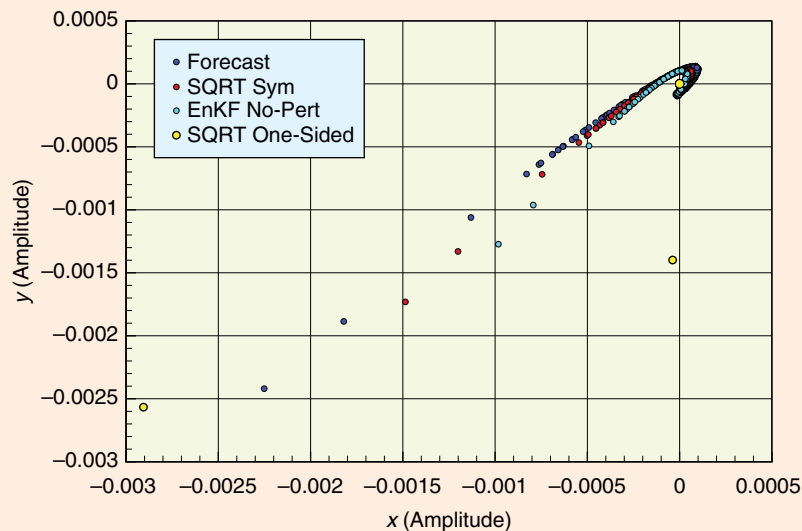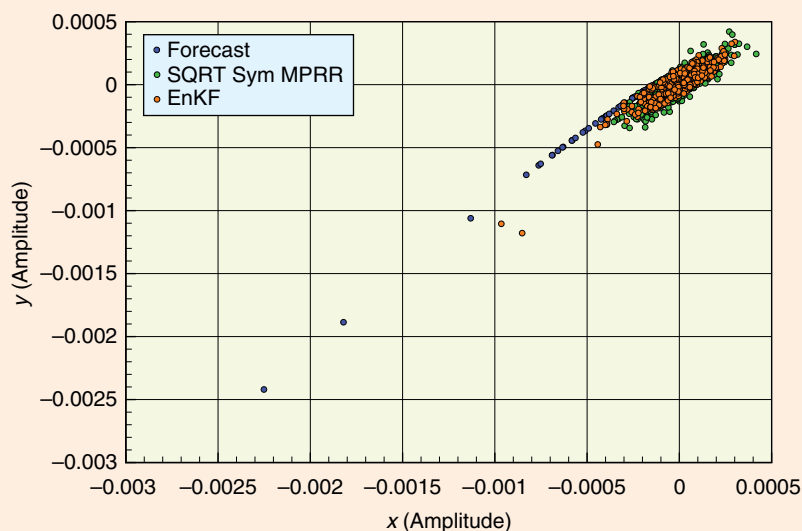
FIGURE 7 Forecast and analysis ensembles for the Lorenz equations illustrating properties of the analysis schemes discussed in the text. The data used in these plots were contributed by Dr. Pavel Sakov.

Gaussian, and some of the non-Gaussian properties of the forecast ensemble is retained, as indicated by the two outliers that represent the tail of the distribution seen in the forecast ensemble.

It is also interesting to consider the standard EnKF scheme when used without perturbation of measurements. It is then clear from (28) that the variance is reduced twice by the additional multiplication with $I - K_e M$ resulting from $C_{\epsilon\epsilon}^e$ in (28) being identical to zero when the measurements are not treated as stochastic variables. Figure 7(a) shows that the EnKF scheme without perturbation of measurements preserves the shape of the forecast distribution in the same

way as the symmetric square root scheme, although the variance is too low. Thus, the perturbation of measurements in EnKF both increases the ensemble variance to the "correct" value, and introduces additional randomization. The randomization is different from the one observed in (76) since only the increments are randomized in the EnKF scheme with perturbation of measurements.

It is currently not clear which of the analysis schemes, that is, the standard EnKF (62), the symmetric square root (75), or the symmetric square root with random rotation (76), is best in practice. Probably the choice of analysis scheme depends on the dynamical model and possibly also on the measurement density and ensemble size used. For a linear dynamical model, the forecast distribution is Gaussian, and the random rotation is not needed. Thus, we then expect the symmetric square root (75) to be the best choice. On the other hand, for a strongly nonlinear dynamical model where non-Gaussian effects are dominant in the predicted ensemble, the symmetric square root with a random rotation (76) or EnKF with perturbed measurements (62) may work better. Both of these schemes introduce Gaussianity into the analysis update, while a Gaussian forecast ensemble may lead to more consistent analysis updates.

The random rotation might be considered as a resampling from a Gaussian distribution at each analysis update. Note again that the random rotation in the square root filter, contrary to the measurement perturbation used in EnKF, completely eliminates all previous non-Gaussian structures that may be contained in the forecast ensemble.

SPURIOUS CORRELATIONS, LOCALIZATION, AND INFLATION

Since EnKF is a Monte Carlo method, making this method affordable for large systems requires the use of a sufficiently small ensemble of model realizations. Around 100 realizations in the ensemble is typical in applications, and in many cases we see only marginal improvements when the ensemble size is further increased, which is explained by the slow convergence, proportional to $\sqrt{N}$, of Monte Carlo methods, together with the fact that a large part of the variability in the state and parameters often is well represented by an ensemble of 100 model realizations. On the other hand, even $\mathcal{O}(100)$ model realizations become extremely computationally demanding in many applications, which is an incentive for using as few realizations as possible. In the following we discuss the problems caused by using a finite ensemble size and present some remedies that can reduce the impact of sampling errors.

Spurious Correlations

The use of a finite ensemble size to approximate the error covariance matrix introduces sampling errors that are seen as spurious correlations over long spatial distances or between variables known to be uncorrelated. A result of these sampling errors is that the updated ensemble variance is underestimated. On the other hand, the consistency of the updated variance improves when a larger ensemble is used. A spurious correlation between a predicted measurement and a variable leads to a small nonphysical update of the variable in each ensemble member, and thus an associated variance reduction. This problem is present in all EnKF applications and can lead to filter divergence.

The following example, which is based on the linear advection case from Figure 2, illustrates the variance reduction resulting from spurious correlations. We use the form (62) for the EnKF analysis scheme with the update matrix X defined from (63).

An additional ensemble $B \in \mathcal{R}^{n_{\text{rand}} \times N}$ is generated, where each row contains random samples from a Gaussian distribution with mean equal to zero and variance equal to one, and the entries in different rows are sampled independently. Thus, B is the ensemble matrix for a state vector of independent variables with zero mean and unit variance. At analysis times we compute the updates

$$\begin{pmatrix} A^{\text{a}} \\ B^{\text{a}} \end{pmatrix} = \begin{pmatrix} A^{\text{f}} \\ B^{\text{f}} \end{pmatrix} X. \tag{77}$$

The predicted ensemble A^{f} is the result of the ensemble integration using the advection model, while B^{f} does not evolve according to any dynamical equation and at an update time equals B^{a} at the previous update time.

Since the correlations between B and the predicted measurement perturbations S become zero in the limit of an infinite ensemble size, it follows that

$$\lim_{N \to \infty} \frac{B S^{\text{T}}}{N - 1} = 0. \tag{78}$$

However, due to the finite ensemble size, (78) cannot be exactly satisfied, and B^{a} experiences a small update and associated reduction of variance through the update in (77).

As in the advection example, we compute the matrix X based on the four measurements, and then apply it to B according to (77) at every analysis time. The value $n_{\text{rand}} = 100$ is found to be sufficient to obtain a consistent result that is independent of the random sampling of B.

The variance reduction resulting from the spurious correlations is illustrated in Figure 8, which shows the decrease of the average variance of the random ensemble **B**, resulting from EnKF with 100 and 250 realizations, and from the symmetric square root scheme using 100 realizations.

EnKF with 100 realizations is repeated five more times using different random seeds to verify that the result is independent of the seed. A nearly linear decrease of variance is obtained during the first 50 updates, while for the final 12 updates the decrease is lower. The reason for the lower error variance reduction in the final part of the experiment is that the information assimilated at one measurement location propagates to the next measurement location during 50 updates. Thus, after 50 updates the ensemble variance is lower at the measurement locations, and the relative weight on the data compared to the prediction is decreased. EnKF with 250 realizations experiences a significantly lower impact from spurious correlations, as expected.

The square root scheme is slightly less influenced by the spurious correlations, and an explanation can be that the measurement perturbations in the EnKF update increases the strength of the update of individual realizations and thus amplifies the impact of the spurious correlations.

In many dynamical systems, the variance decrease caused by spurious correlations may be masked by strong dynamical instabilities. The impact of the spurious correlations may then be less significant. On the other hand, in parameter-estimation problems, the spurious correlations clearly lead to an underestimate of the ensemble variance of the parameters.

Localization

We now discuss the use of localization to reduce spurious correlations [48]. Two classes of localization methods are currently used, covariance localization and local updating.

In [48] the ensemble covariance matrix is multiplied with a specified correlation matrix through a Schur product (entry-wise multiplication). The specified correlation functions are defined with local support and thus effectively truncate the long-range spurious correlations produced by the limited ensemble size. Covariance localization is used in [11], [12], [49], and [50].

We can assume that only measurements located within a certain distance from a gridpoint impact the analysis in that gridpoint. This assumption allows for an algorithm where the analysis is computed gridpoint by gridpoint, and only a subset of observations, located near the current gridpoint, is used in each local analysis. This approach is used in [51], [52], and [37] and is also the approach used in the local EnKF in [53]. In addition to reducing the impact of long-range spurious correlations, the localization methods make it simpler to handle large data sets where the number
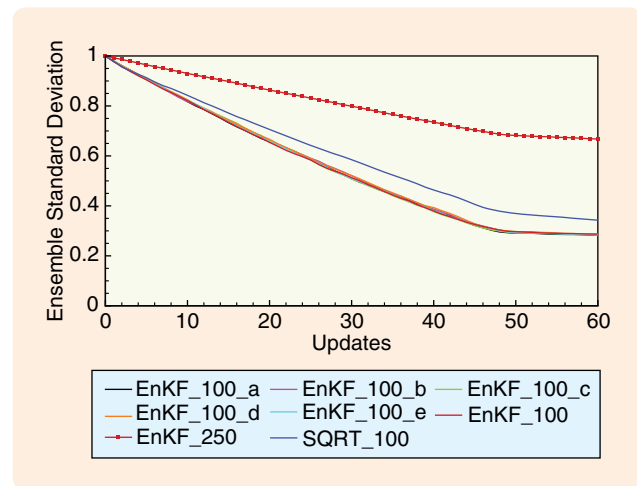

FIGURE 8 Variance reduction of a random ensemble due to spurious correlations, as a function of analysis updates. The ensemble Kalman filter (EnKF) with 100 realizations is compared with EnKF with 250 realizations as well as the square root scheme using 100 realizations. EnKF with 100 realizations is repeated using different seeds to ensure that the results are consistent.

of measurements is much greater than the number of ensemble realizations.

Another reason for computing the local analysis is the fact that EnKF is computed in a space spanned by the ensemble members. This subspace may be rather small compared to the total dimension of the model state. Computing the analysis gridpoint by gridpoint implies that, for each gridpoint, a small model state is solved for in a relatively large ensemble space. The analysis then results from a different combination of ensemble members for each gridpoint, and the analysis scheme is allowed to reach solutions not originally represented by the ensemble. In many applications the local analysis scheme significantly reduces the impact of a limited ensemble size and allows for the use of EnKF with high-dimensional model systems.

The degree of approximation introduced by the local analysis depends on the range of influence defined for the observations. In the limit that this range becomes sufficiently large to include all of the data, the solution for all the gridpoints becomes identical to the standard global analysis. The range parameter must be tuned and should be large enough to include the information from measurements that contribute significantly but small enough to eliminate the spurious impact of remote measurements.

The local analysis algorithm goes as follows. We first construct the input matrices to the global EnKF, that is, the measured ensemble perturbations S, the innovations D', and either the measurement perturbations E or the measurement error covariance matrix $C_{\epsilon\epsilon}$. We then loop through the model grid, and, for each gridpoint, for example, (i, j) for a two-dimensional model, we extract the rows from these matrices corresponding to measurements

that are used in the current update, and then compute the matrix $X_{(i,j)}$ that defines the update for gridpoint (i, j).

The analysis at gridpoint (i, j) becomes

$$A_{(i,j)}^{a} = A_{(i,j)}X_{(i,j)} \tag{79}$$
$$= A_{(i,j)}X + A_{(i,j)}(X_{(i,j)} - X), \tag{80}$$

where X is the global solution, while $X_{(i,j)}$ becomes the solution for a local analysis corresponding to gridpoint (i, j) where only the nearest measurements are used in the analysis. Thus, it is possible to compute the global analysis first and then add the corrections from the local analysis if these effects are significant.

The quality of the EnKF analysis is connected to the ensemble size used. We expect that to achieve the same quality of the result, a larger ensemble is needed for the global analysis than the local analysis. In the global analysis, a large ensemble is needed to properly explore the state space and to provide a consistent result that is as good as the local analysis. Note also that the use of a local analysis scheme is likely to introduce nondynamical modes, although the amplitudes of these modes are small if a large enough influence radius is used when selecting measurements. We also refer to the discussions on localization and filtering of long-range correlations by [54].

In adaptive localization methods, the assimilation system itself is used to determine the localization strategy. Such algorithms are useful since the dynamical covariance functions change in space and time, and the spurious correlations depend on the ensemble size. Thus, every assimilation problem and ensemble size requires a separate tuning of the localization parameters.

The hierarchical approach in [55] uses several small ensembles to explore the need for using localization in the analysis. This approach uses a Monte Carlo method based on splitting the ensemble into several small ensembles to assess the sampling errors and the spurious correlations. This method is a statistically consistent approach to the problem. However, the localization is optimized for a small ensemble and may become suboptimal when used with the full ensemble including all realizations.

An alternative localization method in [56] is based on the online computation of a flow-dependent moderation function that is used to damp long-range and spurious correlations. This method is named SENCORP for "smoothed ensemble correlations raised to a power." The idea is that the moderation functions can be generated from a smoothed covariance function, which, when raised to a power, damps small correlations.

In [57] a local analysis method handles measurements that are integral parameters of the model state. The idea is that the covariance matrix of the predicted measurements is computed globally using the full model state, while the updates are computed locally gridpoint by gridpoint, and only the measurements that have significant correlations with the model variables in the local gridpoint are assimilated.

Thus, while traditional localization methods are distance based, [55]–[57] discuss adaptive localization methods where the assimilation system determines whether correlations are significant or spurious, and whether a particular measurement shall be used in the update of a particular model variable. The further development of adaptive localization methods is important for many applications where distance-based methods are less suitable, an example being the use of measurements that are integral functions of the model state as in [57].

Finally, it is not clear how the local analysis scheme is best implemented in EnKS. One approach is to define the local analysis to use only measurements in a certain space-time domain, taking into account the propagation of information in the model together with the time scales of the model. In [58] EnKS is used with a high-dimensional atmospheric circulation model. The impact of spurious correlations related to the lag time in a lagged EnKS is studied, and it is pointed out that the lagged implementation facilitates localization in time.

Inflation

A covariance inflation procedure [59] can be used to counteract the variance reduction observed due to the impact of spurious correlations as well as other effects leading to underestimation of the ensemble variance. The impact of ensemble size on noise in distant covariances is examined in [49], while the impact of using an "inflation factor" as discussed in [59] is evaluated. The inflation factor is used to replace the forecast ensemble according to

$$\psi_j = \rho(\psi_j - \overline{\psi}) + \overline{\psi}, \tag{81}$$

with ρ slightly greater than one (typically 1.01). The inflation procedure is also used in [60], where the EnKF is examined in an application with the Lorenz attractor, and results are compared with those obtained from different versions of the singular evolutive extended Kalman (SEEK) filter and a particle filter. In [60], ensembles with very few members are used, which favors methods like the SEEK where the "ensemble" of empirical orthogonal functions (EOFs) is selected to best represent the model attractor.

Several approaches adaptively estimate an optimal inflation parameter. In [61] the covariance inflation is estimated based on the sequence of innovation statistics, while in [62] a method is presented that is based on augmenting the inflation parameter to the model state where it is updated as a parameter in the EnKF analysis computations. Online estimation of the inflation parameter is also studied in [63] together with the simultaneous estimation of observation errors. It is found that the estimation of inflation alone does not work appropriately without accurate observation error statistics, and vice versa.

Clearly, the inflation parameter becomes a tuning parameter, and optimally it is best estimated adaptively. The need for inflation depends on the use of a local versus global analysis scheme, and the use of a local scheme can to a large extent reduce the need for an additional inflation.

Here we describe an alternative approach for estimating the inflation coefficient. In the spurious correlation example, as presented in Figure 8, an independent ensemble is used to quantify the variance reduction due to spurious correlations. A simple algorithm for correcting the analyzed ensemble perturbations in each analysis step goes as follows.

At each analysis time we generate the additional ensemble matrix B^f with random normally distributed numbers, such that the mean in each row is exactly zero, and the variance is exactly equal to one. We thus sample the matrix randomly from $\mathcal{N}(0, 1)$. Then, for each row, first subtract any nonzero mean, then compute the standard deviation and scale all entries by it. Then, compute the analysis update according to (77). For each row in B^a, compute the standard deviation. The inflation factor ρ is then defined as one over the average of the standard deviations from each row in B^a. The accuracy of the estimated inflation factor depends on the number of realizations used as well as the number of rows in B. It is expected that with a low number of realizations additional rows in B might compensate for the sampling errors when computing the inflation factor.

This algorithm provides a good first approximation of the inflation factor needed to counteract variance reduction due to long-range spurious correlations resulting from sample noise. The estimated inflation factor depends on the number of realizations used, the number of measurements, and the strength of the update determined by the innovation vector and both the predicted and measurement error covariance matrices. A question remains, as to whether the inflation is best applied equally for the whole model state, including at the measurement locations.

CONCLUSIONS

This article provides a fundamental theoretical basis for understanding EnKF and serves as a useful text for future users. Data assimilation and parameter-estimation problems are explained, and the concept of joint parameter and state estimation, which can be solved using ensemble methods, is presented. KF and EKF are briefly discussed before introducing and deriving EnKF. Similarities and differences between KF and EnKF are pointed out. The benefits of using EnKF with high-dimensional and highly nonlinear dynamical models are illustrated by examples. EnKF and EnKS are also derived from Bayes theorem, using a probabilistic approach. The derivation is based on the assumption that measurement errors are independent in time and the model represents a Markov process, which allows for Bayes theorem to be written in a recursive form, where measurements are processed sequentially in time. The practical implementation of the analysis scheme is discussed, and it is shown that it can be computed efficiently in the space spanned by the ensemble realizations. The square root scheme is discussed as an alternative method that avoids the perturbation of measurements. However, the square root scheme has other pitfalls, and it is recommended to use the symmetric square root with or without a random rotation. The random rotation introduces a stochastic component to the update, and the quality of the scheme may then not improve compared to the original stochastic EnKF scheme with perturbed measurements.

AUTHOR INFORMATION

Geir Evensen (geve@statoilhydro.com) received the Ph.D. in applied mathematics from the University of Bergen, Norway, in 1992. He has published more than 40 articles related to data assimilation, including *Data Assimilation: The Ensemble Kalman Filter*. He currently works on data assimilation and parameter estimation as a research director at StatoilHydro in Bergen and holds an associate position at the Nansen Center in Bergen.

REFERENCES

[1] G. Evensen, "Sequential data assimilation with a nonlinear quasi-geostrophic model using Monte Carlo methods to forecast error statistics," *J. Geophys. Res.*, vol. 99, no. C5, pp. 10143–10162, 1994.
[2] R. E. Kalman, "A new approach to linear filter and prediction problems," *J. Basic Eng.*, vol. 82, pp. 35–45, 1960.
[3] R. E. Kalman and R. S. Bucy, "New results of linear filtering and prediction theory," *J. Basic Eng.*, vol. 83, pp. 95–108, 1961.
[4] O. Talagrand and P. Courtier, "Variational assimilation of meteorological observations with the adjoint vorticity equation. I. Theory," *Q. J. R. Meteorol. Soc.*, vol. 113, pp. 1311–1328, 1987.
[5] E. Kalnay, H. Li, T. Miyoshi, S.-C. Yang, and J. Ballabrera-Poy, "4D-Var or ensemble Kalman filter?," *Tellus A*, vol. 59, pp. 758–773, 2007.
[6] E. J. Fertig, J. Harlim, and B. R. Hunt, "A comparative study of 4D-Var and a 4D ensemble Kalman filter: Perfect model simulations with Lorenz-96," *Tellus A*, vol. 59, pp. 96–101, 2006.
[7] G. Evensen, "Using the extended Kalman filter with a multilayer quasi-geostrophic ocean model," *J. Geophys. Res.*, vol. 97, no. C11, pp. 17905–17924, 1992.
[8] G. Evensen, *Data Assimilation: The Ensemble Kalman Filter.* New York: Springer, 2007.
[9] G. Burgers, P. J. van Leeuwen, and G. Evensen, "Analysis scheme in the ensemble Kalman filter," *Mon. Weather Rev.*, vol. 126, pp. 1719–1724, 1998.
[10] J. L. Anderson, "An ensemble adjustment Kalman filter for data assimilation," *Mon. Weather Rev.*, vol. 129, pp. 2884–2903, 2001.
[11] J. S. Whitaker and T. M. Hamill, "Ensemble data assimilation without perturbed observations," *Mon. Weather Rev.*, vol. 130, pp. 1913–1924, 2002.

[12] C. H. Bishop, B. J. Etherton, and S. J. Majumdar, "Adaptive sampling with the ensemble transform Kalman filter. Part I: Theoretical aspects," *Mon. Weather Rev.*, vol. 129, pp. 420–436, 2001.

[13] M. K. Tippett, J. L. Anderson, C. H. Bishop, T. M. Hamill, and J. S. Whitaker, "Ensemble square-root filters," *Mon. Weather Rev.*, vol. 131, pp. 1485–1490, 2003.

[14] A. Doucet, N. de Freitas, and N. Gordon, Eds. *Sequential Monte Carlo Methods in Practice (Statistics for Engineering and Information Science)*. New York: Springer-Verlag, 2001.

[15] C. L. Keppenne and M. Rienecker, "Initial testing of a massively parallel ensemble Kalman filter with the Poseidon isopycnal ocean general circulation model," *Mon. Weather Rev.*, vol. 130, pp. 2951–2965, 2002.

[16] C. L. Keppenne and M. Rienecker, "Assimilation of temperature into an isopycnal ocean general circulation model using a parallel ensemble Kalman filter," *J. Mar. Syst.*, vol. 40-41, pp. 363–380, 2003.

[17] C. L. Keppenne, M. Rienecker, N. P. Kurkowski, and D. A. Adamec, "Ensemble Kalman filter assimilation of temperature and altimeter data with bias correction and application to seasonal prediction," *Nonlinear Process. Geophys.*, vol. 12, pp. 491–503, 2005.

[18] I. Szunyogh, E. J. Kostelich, G. Gyarmati, D. J. Patil, B. R. Hunt, E. Kalnay, E. Ott, and J. A. Yorke, "Assessing a local ensemble Kalman filter: Perfect model experiments with the national centers for environmental prediction global model," *Tellus A*, vol. 57, pp. 528–545, 2005.

[19] P. L. Houtekamer and H. L. Mitchell, "Ensemble Kalman filtering," *Q. J. R. Meteorol. Soc.*, vol. 131, pp. 3269–3289, 2005.

[20] B. R. Hunt, E. J. Kostelich, and I. Szunyogh, "Efficient data assimilation for spatiotemporal chaos: A local ensemble transform Kalman filter," *Physica D*, vol. 230, pp. 112–126, 2007.

[21] I. Szunyogh, E. J. Kostelich, G. Gyarmati, E. Kalnay, B. R. Hunt, E. Ott, E. Satterfield, and J. A. Yorke, "A local ensemble transform Kalman filter data assimilation system for the NCEP global model," *Tellus A*, vol. 60, pp. 113–130, 2008.

[22] J. S. Whitaker, T. M. Hamill, X. Wei, Y. Song, and Z. Toth, "Ensemble data assimilation with the NCEP global forecast system," *Mon. Weather Rev.*, vol. 136, pp. 463–482, 2008.

[23] K. Eben, P. Juru, J. Resler, M. Belda, E. Pelikán, B. C. Krger, and J. Keder, "An ensemble Kalman filter for short-term forecasting of tropospheric ozone concentrations," *Q. J. R. Meteorol. Soc.*, vol. 131, pp. 3313–3322, 2005.

[24] O. Barrero Mendoza, B. De Moor, and D. S. Bernstein, "Data assimilation for magnetohydrodynamics systems," *J. Comput. Appl. Math.*, vol. 189, no. 1, pp. 242–259, 2006.

[25] Y. Zhou, D. McLaughlin, and D. Entekhabi, "An ensemble-based smoother with retrospectively updated weights for highly nonlinear systems," *Mon. Weather Rev.*, vol. 135, pp. 186–202, 2007.

[26] M. Eknes and G. Evensen, "Parameter estimation solving a weak constraint variational formulation for an Ekman model," *J. Geophys. Res.*, vol. 102, no. C6, pp. 12479–12491, 1997.

[27] J. C. Muccino and A. F. Bennett, "Generalized inversion of the Korteweg-de Vries equation," *Dyn. Atmos. Oceans*, vol. 35, pp. 227–263, 2001.

[28] A. F. Bennett, *Inverse Methods in Physical Oceanography*. Cambridge, U.K.: Cambridge Univ. Press, 1992.

[29] A. F. Bennett, *Inverse Modeling of the Ocean and Atmosphere*. Cambridge, U.K.: Cambridge Univ. Press, 2002.

[30] G. Evensen, J. Hove, H. C. Meisingset, E. Reiso, K. S. Seim, and Ø. Espelid, "Using the EnKF for assisted history matching of a North Sea reservoir model," Houston, TX, Soc. Petroleum Eng., Inc., SPE 106184, 2007.

[31] R. N. Miller, "Perspectives on advanced data assimilation in strongly nonlinear systems," in *Data Assimilation: Tools for Modelling the Ocean in a Global Change Perspective (NATO ASI, vol. I 19)*, P. P. Brasseur and J. C. J. Nihoul, Eds. Berlin: Springer-Verlag, 1994, pp. 195–216.

[32] R. N. Miller, M. Ghil, and F. Gauthiez, "Advanced data assimilation in strongly nonlinear dynamical systems," *J. Atmos. Sci.*, vol. 51, pp. 1037–1056, 1994.

[33] P. Gauthier, P. Courtier, and P. Moll, "Assimilation of simulated wind lidar data with a Kalman filter," *Mon. Weather Rev.*, vol. 121, pp. 1803–1820, 1993.

[34] F. Bouttier, "A dynamical estimation of forecast error covariances in an assimilation system," Mon. Weather Rev., vol. 122, pp. 2376–2390, 1994.

[35] A. H. Jazwinski, *Stochastic Processes and Filtering Theory*. San Diego, CA: Academic, 1970.

[36] R. H. Reichle, D. B. McLaughlin, and D. Entekhabi, "Hydrologic data assimilation with the ensemble Kalman filter," *Mon. Weather Rev.*, vol. 130, pp. 103–114, 2002.

[37] G. Evensen, "The ensemble Kalman filter: Theoretical formulation and practical implementation," *Ocean Dyn.*, vol. 53, pp. 343–367, 2003.

[38] G. Evensen and P. J. van Leeuwen, "An ensemble Kalman smoother for nonlinear dynamics," *Mon. Weather Rev.*, vol. 128, pp. 1852–1867, 2000.

[39] P. J. van Leeuwen and G. Evensen, "Data assimilation and inverse methods in terms of a probabilistic formulation," *Mon. Weather Rev.*, vol. 124, pp. 2898–2913, 1996.

[40] G. Evensen, "Advanced data assimilation for strongly nonlinear dynamics," *Mon. Weather Rev.*, vol. 125, pp. 1342–1354, 1997.

[41] E. N. Lorenz, "Deterministic nonperiodic flow," *J. Atmos. Sci.*, vol. 20, pp. 130–141, 1963.

[42] G. Evensen, "Sampling strategies and square root analysis schemes for the EnKF," *Ocean Dyn.*, vol. 54, pp. 539–560, 2004.

[43] O. Leeuwenburgh, "Assimilation of along-track altimeter data in the Tropical Pacific region of a global OGCM ensemble," *Q. J. R. Meteorol. Soc.*, vol. 131, pp. 2455–2472, 2005.

[44] P. Sakov and P. R. Oke, "Implications of the form of the ensemble transform in the ensemble square root filters," *Mon. Weather Rev.*, vol. 136, no. 3, pp. 1042–1053, 2008.

[45] X. Wang, C. H. Bishop, and S. J. Julier, "Which is better, an ensemble of positive-negative pairs or a centered spherical simplex ensemble," *Mon. Weather Rev.*, vol. 132, pp. 1590–1605, 2004.

[46] O. Leeuwenburgh, G. Evensen, and L. Bertino, "The impact of ensemble filter definition on the assimilation of temperature profiles in the Tropical Pacific," *Q. J. R. Meteorol. Soc.*, vol. 131, pp. 3291–3300, 2005.

[47] D. M Livings, S. L. Dance, and N. K. Nichols, "Unbiased ensemble square root filters," *Physica D*, vol. 237, pp. 1021–1028, 2008.

[48] P. L. Houtekamer and H. L. Mitchell, "A sequential ensemble Kalman filter for atmospheric data assimilation," *Mon. Weather Rev.*, vol. 129, pp. 123–137, 2001.

[49] T. M. Hamill, J. S. Whitaker, and C. Snyder, "Distance-dependent filtering of background error covariance estimates in an ensemble Kalman filter," *Mon. Weather Rev.*, vol. 129, pp. 2776–2790, 2001.

[50] J. L. Anderson, "A local least squares framework for ensemble filtering," *Mon. Weather Rev.*, vol. 131, pp. 634–642, 2003.

[51] V. E. Haugen and G. Evensen, "Assimilation of SLA and SST data into an OGCM for the Indian ocean," *Ocean Dyn.*, vol. 52, pp. 133–151, 2002.

[52] K. Brusdal, J. M. Brankart, G. Halberstadt, G. Evensen, P. Brasseur, P. J. van Leeuwen, E. Dombrowsky, and J. Verron, "An evaluation of ensemble based assimilation methods with a layered OGCM," *J. Mar. Syst.*, vol. 40-41, pp. 253–289, 2003.

[53] E. Ott, B. Hunt, I. Szunyogh, A. V. Zimin, E. Kostelich, M. Corazza, E. Kalnay, D. J. Patil, and J. A. Yorke, "A local ensemble Kalman filter for atmospheric data assimilation," *Tellus A*, vol. 56, pp. 415–428, 2004.

[54] H. L. Mitchell, P. L. Houtekamer, and G. Pellerin, "Ensemble size, and model-error representation in an ensemble Kalman filter," *Mon. Weather Rev.*, vol. 130, pp. 2791–2808, 2002.

[55] J. L. Anderson, "Exploring the need for localization in the ensemble data assimilation using a hierarchical ensemble filter," *Physica D*, vol. 230, pp. 99–111, 2007.

[56] C. H. Bishop and D. Hodyss, "Flow-adaptive moderation of spurious ensemble correlations and its use in ensemble-based data assimilation," *Q. J. R. Meteorol. Soc.*, vol. 133, pp. 2029–2044, 2007.

[57] E. J. Fertig, B. R. Hunt, E. Ott, and I. Szunyogh, "Assimilating nonlocal observations with a local ensemble Kalman filter," *Tellus A*, vol. 59, pp. 719–730, 2007.

[58] S. P. Khare, J. L. Anderson, T. J. Hoar, and D. Nychka, "An investigation into the application of an ensemble Kalman smoother to high-dimensional geophysical systems," *Tellus A*, vol. 60, pp. 97–112, 2008.

[59] J. L. Anderson and S. L. Anderson, "A Monte Carlo implementation of the nonlinear filtering problem to produce ensemble assimilations and forecasts," *Mon. Weather Rev.*, vol. 127, pp. 2741–2758, 1999.

[60] D. T. Pham, "Stochastic methods for sequential data assimilation in strongly nonlinear systems," *Mon. Weather Rev.*, vol. 129, pp. 1194–1207, 2001.

[61] X. Wang and C. H. Bishop, "A comparison of breeding and ensemble transform Kalman filter ensemble forecast schemes," *J. Atmos. Sci.*, vol. 60, pp. 1140–1158, 2003.

[62] J. L. Anderson, "An adaptive covariance inflation error correction algorithm for ensemble filters," Tellus A, vol. 59, pp. 210–224, 2007.

[63] H. Li, E. Kalnay, and T. Miyoshi, "Simultaneous estimation of covariance inflation and observation errors within ensemble Kalman filter," *Q. J. R. Meteorol. Soc.*, vol. 135, no. 639, pp. 523–533, 2009.